

CHARACTERIZING THE MACROPHAGE RESPONSE TO PERIPHERAL NERVE INJURY

Thesis

Presented to the Faculty of the Graduate School

Of Cornell University

In Partial Fulfillment of the Requirements for the Degree of

Master of Science

By

Megan Bernard

February 2016

ABSTRACT

Recovery after peripheral nerve injury (PNI) is slow and often incomplete. Nerve graft offers a promising therapy for improving functional recovery after repair. Increasing Schwann cell migration and modulating macrophage phenotype can improve nerve regeneration by using endogenous tissue repair mechanisms to create a more robust growth-permissive environment. Here we investigate the modulation of macrophage phenotype using a peripheral nerve-specific extracellular matrix (NSECM) at the site of peripheral nerve injury. The effects of NSECM on macrophage gene expression were evaluated *in vitro*. Results demonstrate that NSECM promotes a distinct phenotype compared to known phenotypes of classically (M1) and alternatively (M2) activated macrophages. The effects of NSECM on macrophage accumulation in the injured nerve, motor neuron regeneration, and *in vivo* macrophage gene expression were also evaluated. Murine sciatic nerves were transected and repaired using nerve conduits alone or conduits filled with NSECM or 0.7% agarose. Immunohistochemical evaluation of macrophage accumulation in the injured nerve at 5 days after repair showed that M1 macrophage populations decreased with NSECM treatment, but M2 macrophage populations did not change, compared to control (empty). FACS was used to isolate macrophages from the injured nerve at different time points after repair and gene expression analysis was performed to characterize changes in macrophage phenotype associated with time after injury and experimental group. Our results showed that macrophages express M2 genes early after injury, followed by development of M1-like genes later. These changes were more profound in macrophages treated with agarose. Macrophages treated with NSECM showed less variation over time. We also evaluated functional recovery by quantifying motor neuron regeneration at different time points after injury, and although we saw progression of recovery from 2-8 weeks after injury, experimental groups did not affect functional regeneration in the mouse. Taken together, our results show improvement over previously used immunohistochemical methods for

evaluating macrophage populations by use of FACS and high throughput gene expression analyses. In addition, we found that, in contrast to previous findings, NSECM does not improve functional regeneration of the murine peripheral nerve.

BIOGRAPHICAL SKETCH

Megan Bernard is currently a first year graduate student in Cornell University's Comparative Biological Sciences master's program. She graduated *summa cum laude* from the University of Massachusetts with a bachelor's degree in pre-veterinary medicine. In 2013 she matriculated at Cornell University College of Veterinary Medicine, and took a leave of absence in 2015 to pursue research in the graduate school under the NYSTEM training grant. In February 2016, she will graduate with a master's degree and return to the professional veterinary medicine curriculum with the class of 2018. Ms. Bernard is a member of a number of professional and academic organizations, including the student chapter of the American Veterinary Medical Association (SCAVMA), the student chapter of the American Association of Small Ruminant Practitioners (AASRP), the student chapter of the American Association of Bovine Practitioners (AABP), and the student chapter of the American Association of Equine Practitioners (AAEP).

ACKNOWLEDGMENTS

I would like to acknowledge Dr. Jonathan Cheetham, Dr. Joy Tomlinson, Travis Prest, Dr. Bryan Brown, Timothy Moore, Emilija Zygelyte, and Yutao Su for their contributions and assistance with this project.

I would like to acknowledge Lynn Johnson at the Cornell Statistical Consulting Unit as well as Mike Sledziona for their assistance with data analysis.

I would like to acknowledge Dorian LaTocha and Cornell's Flow Cytometry Core Facility for assistance with flow cytometric analysis and cell sorting. Cytometry core is supported in part by the ESSCF, NYS-DOH, Contract #C026718. Opinions expressed are solely of the author; they do not necessarily reflect the view of ESSCB, the NYS-DOG, or NYS.

I would like to acknowledge the Molecular Biology Core Facility at the Geisel School of Medicine at the University of Dartmouth for performing gene expression analyses.

Additionally, I would like to acknowledge funding from New York Stem Cell Science (NYSTEM) as well as NIH.

TABLE OF CONTENTS

Contents

BIOGRAPHICAL SKETCH	iii
ACKNOWLEDGMENTS	iv
INTRODUCTION	1
MATERIALS & METHODS	1
RESULTS.....	17
Bone Marrow Derived Macrophage Culture	17
Macrophage Immunohistochemistry	26
Macrophage Sorting	27
In Vivo Macrophage Gene Expression Analysis	28
Retrograde Labeling of Regenerated Motor Neurons	35
DISCUSSION.....	37
APPENDIX.....	43
REFERENCES	51

INTRODUCTION

Peripheral nerve injury (PNI) affects approximately 360,000 Americans and 300,000 Europeans annually (Li et al., 2014; Noble, Munro, Prasad, & Midha, 1998). Cases are primarily traumatic in origin, with iatrogenic surgical injury contributing to a notable percentage of cases (7.5%) (Kouyoumdjian, 2006; Portincasa et al., 2007; Scholz et al., 2009). Young men are affected at higher rates (74%) (Noble et al., 1998; Taylor, Braza, Rice, & Dillingham, 2008). In addition to motor dysfunction, PNI is frequently complicated by neuropathic pain, which can be a significant source of morbidity (Pfister et al., 2011). PNI represents a significant cost in the healthcare industry as at least half of all patients require medical and rehabilitation services (Selecki, Ring, Simpson, Vanderfield, & Sewell, 1982).

Despite the large volume of research in peripheral nerve regeneration and advances made in microsurgical techniques, functional outcomes after repair of severe injuries are often disappointing and full functional recovery is seldom achieved (Mackinnon, Doolabh, Novak, & Trulock, 2001; Nichols et al., 2004). Peripheral nerves have some capability to regenerate, reinnervate a target organ and allow the patient to regain function (Deumens et al., 2010; Lundborg et al., 1982; Scholz et al., 2009). The degree of repair, however, is highly dependent on the type and extent of a given nerve injury (Seddon, Medawar, & Smith, 1943) and any delay prior to surgical intervention (S Y Fu & Gordon, 1995). There is a definite need to improve peripheral nerve regeneration, especially after chronic injury.

The processes following PNI are orchestrated and predictable (figure 1). After axotomy the distal nerve stump and a portion of the proximal stump undergo Wallerian degeneration, which cleans up debris which would prevent axon regeneration (Corfas, Velardez, Ko, Ratner, & Peles, 2004; Susan Y. Fu & Gordon, 1997; Gaudet, Popovich, & Ramer, 2011; Waller, 1850). Two key players in the process of Wallerian degeneration and subsequent neural regeneration are

macrophages and Schwann cells (SC). These two cell types are essential in the degenerative and regenerative processes that occur after nerve injury, mediating the environment through which axons can regenerate and make contact with their reinnervation target. Because of their key roles in influencing the outcome of regeneration, macrophages and SCs represent an area of focus in research on peripheral nerve regeneration (Bell & Haycock, 2012; Beuche & Friede, 1984; Sridharan, Cameron, Kelly, Kearney, & Brien, 2015).

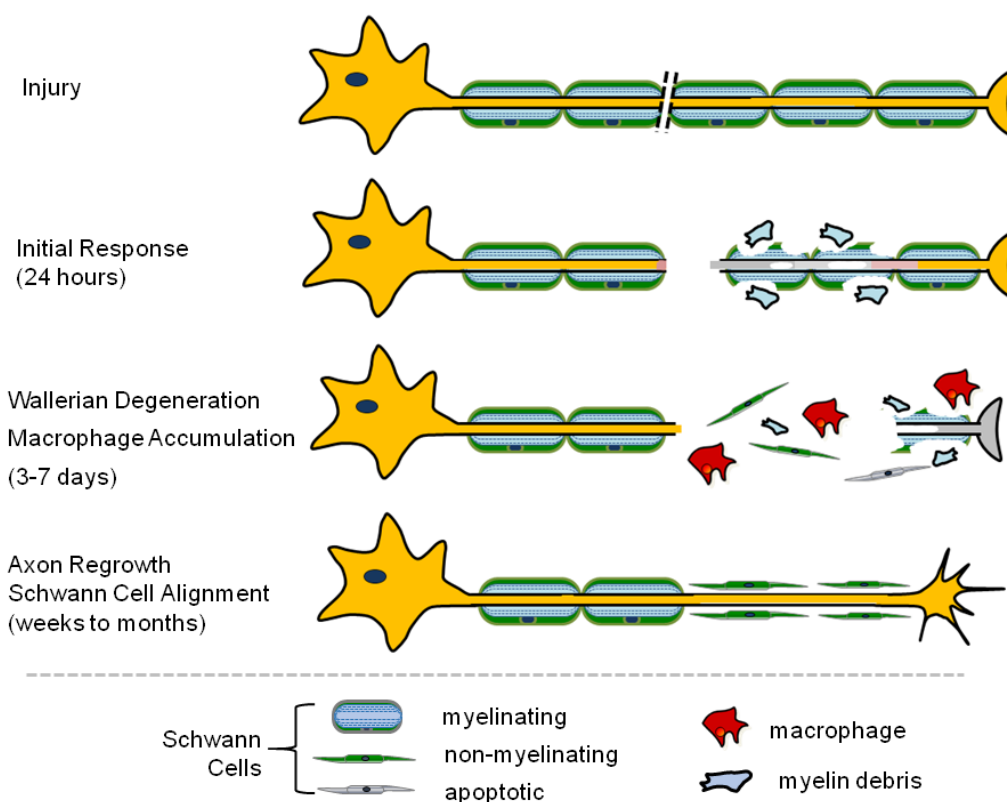


Figure 1: Schematic of the progression of nerve injury to regeneration

Schwann cells, the glial cells of the peripheral nervous system, are intimately associated with neurons. In the uninjured nerve, SC perform several homeostatic functions. They regulate the environment around neurons, providing trophic support and maintaining the blood-nerve barrier and other structural tissue architecture, and they allow saltatory impulse conduction down the length of myelinated axons (Jessen & Mirsky, 2005). In the injured nerve, they have two main

functions. First, they phagocytose debris at the onset of Wallerian degeneration (Gaudet et al., 2011; Waller, 1850). Second, they support the extracellular matrix (ECM) scaffold, growth factors, and chemotactic signals that guide regenerating axons (Bailey, Eichler, Villadiego, & Rich, 1993; Cornbrooks, Carey, McDonald, Timpl, & Bunge, 1983; Scheib & Höke, 2013). To do this, SCs proliferate and migrate across the regenerative bridge between the proximal and distal stumps. As the regenerating axons come into contact with the SCs, the neuron receives SC-secreted neurotrophins which promote continued growth, and the SCs receive neuronal signals that drive differentiation to a myelinating phenotype (Frostick, Yin, & Kemp, 1998). If repair is delayed, the denervated SCs in the distal stump begin to downregulate genes needed to support cell survival and axon regeneration; many will apoptose or become recalcitrant to reinnervation by regenerating neurons' axons (Susan Y. Fu & Gordon, 1997; Gordon, Tyreman, & Raji, 2011; Sulaiman & Gordon, 2000; Taskinen & Røytta, 1997). This is a major reason why nerves that are chronically injured have significantly decreased functional recovery (Gordon et al., 2011).

Macrophages are essential to support and coordinate the role of SC in peripheral nerve repair. By five to seven days after injury, macrophages recruited from the blood monocyte population occupy up to 35% of the cellular population at the injury site (Cattin et al., 2015; P. Chen, Piao, & Bonaldo, 2015; Mueller et al., 2003; Taskinen & Røytta, 1997). Hematogenous and resident macrophages begin to proliferate and secrete inflammatory cytokines and chemokines. This initial inflammation breaks down the blood-nerve barrier, allowing the influx of more immune cells to augment Wallerian degeneration. Macrophage migration into the nerve injury site may be more important than proliferation of resident macrophages and occurs in response to a range of mediators such as IL-10, IL-6, monocyte chemoattractant protein (MCP-1), and leukemia inhibitory factor (LIF) produced by resident SC and macrophages (Mueller et al., 2003; Perrin, Lacroix, Avilés-Trigueros, & David, 2005; Shamash, Reichert, & Rotshenker, 2002; Subang &

Richardson, 2001; Taskinen et al., 2000; Toews, Barrett, & Morell, 1998; Tofaris, Patterson, Jessen, & Mirsky, 2002). These infiltrating macrophages provide 5 major functions. First, they encourage proliferation, activation, and de-differentiation of SC to the non-myelinating phenotype necessary for the repair process by secretion of cytokines such as IL1 (Baichwal, Bigbee, & DeVries, 1988; P. Chen et al., 2015; Gaudet et al., 2011; Heumann et al., 1987; Lindholm, Heumann, Meyer, & Thoenen, 1987; Taskinen & Røyttä, 1997). Second, macrophages together with SC, phagocytose myelin debris, severed axons, and other inhibitory proteins, leaving the extracellular matrix components intact. Third, they respond to local tissue hypoxia in the injured tissues, by releasing VEGF-A, which mediates the formation of a microcapillary network along which SC can migrate (Barrette et al., 2008; Cattin et al., 2015). Fourth, macrophages contribute to tissue regeneration by secreting neurotrophic factors such as Nerve Growth Factor (NGF), which promote axon regeneration (Elkabes, DiCicco-Bloom, & Black, 1996; Gaudet et al., 2011; Lindholm et al., 1987). Fifth, they remodel the regenerating tissues to prevent scar formation and encourage functional tissue architecture (Gaudet et al., 2011; Taskinen & Røyttä, 1997).

Activated macrophages can take on a spectrum of phenotypic profiles that have broadly pro-inflammatory to pro-regenerative effects on tissues. The phenotypes can be categorized *in vitro* as M1 or M2 macrophages and M2 phenotypes can be sub-classified as M2a, M2b, and M2c (Martinez & Gordon, 2014; Murray et al., 2014). These categories represent extremes on a continuum of macrophage phenotypes (figure 2). M1 macrophages are considered to be pro-inflammatory, and can be activated to this state with signals from TH1 lymphocytes like interferon gamma (IFN γ) or tumor necrosis factor (TNF) or by pathogen-associated molecular patterns like lipopolysaccharide (LPS). These macrophages are characterized by expression of inducible nitric oxide synthase (Nos2) and cyclooxygenase 2 (COX-2), two enzymes involved in the production of inflammatory products (Murray et al., 2014). M2 macrophages are considered

to be anti-inflammatory or pro-regenerative. This phenotype can be elicited with products from TH2 or T-regulatory lymphocytes, like IL-4, IL-10, or IL-13. These macrophages are characterized by expression of a mannose receptor (MRC1/CD206), arginase 1 enzyme (Arg1), and the transcription factor peroxisomal proliferator activated receptor gamma (PPAR γ), which are all associated with growth, immune modulation, and repair (Martinez & Gordon, 2014; Murray et al., 2014).



Figure 2: Macrophage phenotype exists on a spectrum with two extremes representing the classically activated (M1, pro-inflammatory) and alternatively activated (M2, pro-regenerative) macrophages.

Manipulation of macrophage phenotype toward an M2 state has the potential to improve peripheral nerve regeneration by recruiting autogenous tissue repair mechanisms and creating a microenvironment which promotes axonal recovery (Bell & Haycock, 2012; Griffin, Hogan, Chhabra, & Deal, 2013; Pfister et al., 2011; Scholz et al., 2009). Recently, Mokarram *et al* demonstrated that polarizing macrophages to an M2 phenotype using IL-4 in the rat increased SC migration and axon sprouting after sciatic transection, compared to using IFN γ to polarize toward M1 macrophages (Mokarram, Merchant, Mukhatyar, Patel, & Bellamkonda, 2012). This introduced the concept of a “regenerative bias” as the ratio of M2 to M1 macrophages, and suggest that modulation of macrophage activity may consequentially lead to control of the downstream events of inflammation and repair in a variety of tissues (Mokarram et al., 2012).

An alternative method of manipulating macrophage phenotype at the site of tissue repair has been through the use of extracellular matrix (ECM) biomaterials which have the advantage of simultaneously providing a scaffold for cell migration (Brown et al., 2012; Brown, Valentin, Stewart-akers, McCabe, & Badylak, 2009; Reing et al., 2009). Extracellular matrix biomaterials, typically derived from porcine urinary bladder and small intestine, have been used in a variety of preclinical and clinical applications for tissue reconstruction and have shown promise as therapies in regenerative medicine (Badylak, 2004; Brown et al., 2011, 2009). The ECM represents the secreted products of cells residing in tissues; it consequently influences cellular behaviors like activation state, attachment, migration, and organization and has been demonstrated to orchestrate cellular functions during regeneration. Extracellular matrix-induced changes to the host regenerative response can be credited to factors released from the ECM as it is degraded by the host (Brown et al., 2012; Reing et al., 2009); The specificity of the process of peripheral nerve repair is enhanced by ECM components such as laminin which enhances SC migration and axon extension across a repair site as well as chemotactic and chemotrophic factors to guide immune cell function (Y. Y. Chen et al., 2005; Ghalib, Houst'ava, Haninec, & Dubovy, 2001; Hall, 1986a, 1986b, 1989; Khuong et al., 2014; Lavasani et al., 2014). It has been shown that these ECM biomaterials can modulate the spatiotemporal relationships of M1 and M2 macrophages and microglia in the central nervous system (Ren, van der Merwe, & Steketee, 2015).

Recently, production of a nerve-specific extracellular matrix hydrogel (NSECM) for use in nerve repair was described [Prest *et al* 2015, in review]. Nerve specific ECM produced by decellularizing porcine sciatic nerve maintains basement membrane components such as native collagen IV, hyaluronic acid, glycosaminoglycans, as well as neurotrophins such as nerve growth factor (NGF) and ciliary neurotrophic factor (CNTF). Decellularization also removes

myelin and at least 85% of dsDNA content, which inhibit nerve regeneration (Prest *et al* 2015, in review).

The current project aims to improve peripheral nerve regeneration by using NSECM to modulate the macrophage and SC responses to nerve injury in the mouse. We hypothesized that NSECM would promote a macrophage pro-regenerative phenotype and increase the number of motor neurons extending their axons across the site of repair.

MATERIALS & METHODS

Overview of methods

To evaluate the effects of NSECM on macrophage function and nerve regeneration, both quantitative and qualitative outcome measures were employed. The effects of NSECM on macrophage polarization *in vitro* were assessed using flow cytometric and gene expression analysis of cultured macrophages. *In vivo* cell macrophage populations were isolated from injured sciatic nerve using fluorescence activated cell sorting (FACS) at time points representing early, mid, and late stages of macrophage migration to the site of injury. Gene expression of sorted cells was evaluated using NanoString™ nCounter technology. Accumulation of M1 and M2 macrophages was determined using immunohistochemistry. Motor neuron regeneration was quantified using retrograde labeling.

The following experiments evaluating macrophage populations were reported according to guidelines described by Martinez and Gordon, 2014. As stated above, macrophages exist in pleiotropic populations, and although problematic to use the M1/M2 paradigm of macrophage phenotype and function, it provides a useful framework by which to characterize immune responses. Thus, we have selected a variety of outcome measures to evaluate macrophage populations both *in vitro* and *in vivo*. By using immunohistochemistry and flow cytometry, we can evaluate a proportion of macrophages based on selected M1 and M2 markers and extrapolate a generalized function for the whole population. By using gene expression analysis, we are able to evaluate a more accurate depiction of the heterogeneous nature of macrophage populations in the injured nerve.

Bone Marrow-Derived Macrophage Culture and Polarization

The effects of NSECM on cultured macrophages were compared to known immune ligands used to polarized *in vivo* macrophages towards distinct M1 (classically activated) or M2 (alternatively activated) phenotypes. Mice were euthanized by CO₂ inhalation and the skin over the pelvic limbs removed and the coxofemoral, stifle, and tibiotarsal joints disarticulated. The muscle layers were gently removed from the bones to expose the femur and the tibia and fibula. The harvested long bones were then placed in R10 cell culture medium (RPMI 1640 (Corning) with 10% FBS (ThermoFischer), 1% Penicillin/Streptomycin (ThermoFischer), and 1% HEPES (Sigma Aldrich)) and all further bone marrow harvesting was carried out under a biosafety hood. Using sterile forceps, the bones were transferred first to 70% ethanol for 1 minute, then into PBS. The long bones were then cut at the metaphysis to expose the marrow cavity, which was flushed with 2-5mL of sterile PBS, and marrow was collected in a conical tube. The marrow was dispersed by aspirating and expelling through a 20g needle twice. The marrow was centrifuged at 300g for 5 minutes, then resuspended in 5mL red blood cell lysis buffer (eBioscience). Red blood cell lysis was carried out for 5 minutes on ice, and the reaction was quenched with 20mL PBS. The marrow was centrifuged at 300g for 5 minutes and resuspended in R10 cell culture medium, then cells were counted using a hemacytometer and 500,000 cells were plated onto each 100mm sterile polystyrene petri dish (Falcon) with 12mL R10 cell culture medium. Cells were stimulated to differentiate with 10ng/mL macrophage colony stimulating factor (M-CSF, eBioscience). Cells were fed by adding 12mL R10 cell culture medium with 10ng/mL M-CSF (day 3).

On days 6 and 7, cells were polarized toward known *in vitro* phenotypes with IFN γ and LPS (M1) or IL-4 (M2) (Murray et al., 2014) or were stimulated by adding NSECM. No additional cytokines were added for M0 macrophages. On day 6, old media was removed from all plates and replaced with 12 mL fresh R10 media plus 10ng/mL M-CSF. Ligands known to produce

particular extremes of the macrophage polarization spectrum were added to provide known controls: 50ng/mL IFN γ (eBioscience) followed by 100ng/mL LPS on day 7 for M1 polarization; 50ng/mL IL-4 for M2 polarization on day 7; and NSECM at 100, 300, 500, and 700 μ g/mL on day 7. Cells were then harvested for flow cytometry and RNA isolation (day 8).

Cell Harvest

All plates were digested with 0.5mg/mL collagenase type 1 (Sigma) and 0.25mg/mL hyaluronidase (Sigma) buffered with 250 μ L HEPES for 30 minutes at 37°C to break down the NSECM in media and harvest cells that had seeded the NSECM matrix in cell culture. Media was collected and replaced with PBS and the plates were allowed to incubate for another 30 minutes. Plates were then washed three times with PBS; all PBS was collected and added to the previously harvested media. Cell solutions were centrifuged at 300g for 10 minutes and the pellet was resuspended in 0.1% BSA in DPBS. Cells were counted using a hemacytometer and 1.2×10^6 cells were plated on a v-bottom 96-well plate (Nunc, Fischer Scientific) for flow cytometry staining. 2.0×10^5 cells were collected in DNase-free, low-bind eppendorf tubes (Zymogen) for RNA extraction.

Flow Cytometric Analysis of Bone Marrow Derived Macrophages

Bone marrow derived macrophages were stained for flow cytometric analysis. Antibodies and dilutions are listed in Table 1. Dilutions were determined by careful titration. Cells were first stained for viability with Zombie aqua for 15 minutes at room temperature. Washing steps were performed with DPBS. Then cells were incubated with surface markers for 45 minutes at 4°C; washing steps were performed with 0.1% BSA in DPBS. Cells were then fixed and permeabilized with Cytofix/Cytoperm (BD Bioscience) for 20 minutes at 4°C. Once fixed, cells were incubated with intracellular markers for 60 minutes at 4°C. The remaining wash steps were

performed with 1xPerm/Wash in DI water (BD Bioscience). After staining, cells were resuspended in 0.1% BSA in DPBS for analysis.

The stained cells were analyzed on the FACS Aria III (BD Biosciences) using FACS Diva software (BD Biosciences, version 6.1.3) and final analysis was performed with FloJo software (TreeStar v10). Fluorochromes were excited with the instrument's 405nm, 532nm, and 633nm lasers. The appropriate detection filters were used (Table 2). Compensation beads (OneComp, eBioscience) were used to set the compensation matrix. Fluorescence was determined by gating against appropriate controls (unstained, fluorescence minus one) on samples prepared in parallel. Gates were set such that less than 1% positive events were recorded when acquiring the corresponding negative control. Cells were gated on forward and side scatter for general cell size, forward scatter height and width to exclude doublets, and side scatter and Zombie Aqua to exclude dead cells. Macrophages were defined as all viable single cells that were CD11b⁺CD16/32⁺. M1 macrophages were defined as CD11b⁺CD16/32⁺Nos2⁺ and M2 macrophages were defined as CD11b⁺CD16/32⁺Arg1⁺Nos2⁻.

Table 1: Antibodies used for cultured cell staining

Label and clone	Dilution	Conjugate	Distributor & catalog number	Label	Specificity	Diluent
Cd16/32 clone 93	1:50	BV-605	Biolegend 101302	Surface	Pan macrophage	0.1% BSA
Cd11b clone M1/70	1:200	Pacific Blue	eBioscience 14-0112-82	Surface	Pan macrophage	0.1% BSA
iNos2 clone N-20	1:200	APC	Santa Cruz Biotechnology sc-651	Intracellular	M1	1xPerm/Wash
Arginase	1:20	PE	R&D Systems IC5868P	Intracellular	M2	1xPerm/Wash
Zombie Aqua	1:200		BioLegend 423102	Intracellular	Viability	DPBS

Table 2: Excitation and detection settings for antibodies and conjugates used.

Antibody target	Conjugate	Excitation laser (nm)	Filters	Mirror
F4/80	PE-Cy7	532	780/40	740LP
CD11b	Pacific Blue	405	450/50	
CD16/32	BV605	405	585/42	570LP
Nos2	APC	633	660/20	
Arg1	PE	532	575/25	
CD14	PE	532	575/25	
CD19	APC	633	660/20	
CD3e	APC	633	660/20	
Ly6G	APC	633	660/20	
SiglecF	APC	633	660/20	
Ter119	APC	633	660/20	
CD31	APC	633	660/20	
Thy-1	APC	633	660/20	
P75-NGFR	FITC	488	515/20	505LP
Zombie Aqua	n/a	405	525/50	495LP
Propidium iodide	n/a	532	660/20	640LP

RNA Extraction

RNA extraction was performed per Zymogen mini prep© protocol. Briefly, cells were pelleted and resuspended in lysis buffer and put on ice. After lysing, 100% ethanol was added, and all following steps were performed at room temperature. The lysate was filtered through a spin column at 1200g for 45 seconds and the column was washed with wash buffer and spun again. DNA was digested with DNase I enzyme for 15 minutes at room temperature. After a series of washes with prep buffer and wash buffer, RNA was eluted from the spin column with 15 µL RNase-free water. RNA quantity was measured using NanoDrop Lite (Thermo Scientific). RNA extracts were stored at -80°C until processing for RNA expression analysis.

RNA Expression Analysis

To quantify gene expression, the extracted RNA was incubated with a panel of 90 bar-coded probes (Nanostring Technologies, Seattle, WA) specific for genes associated with macrophage phenotype and function (Nanostring Technologies, Seattle, WA). Biological triplicates were run by the Molecular Biology Core Facility at Geisel School of Medicine at Dartmouth (Hanover, NH). Nanostring nSolver Analysis Software (NanoString Technologies) was used to normalize raw data and normalized data was analyzed using JMP Pro 11 software (SAS).

Ethics Statement

Animal studies were performed in accordance with the PHS Policy on Humane Care and Use of Laboratory Animals, the NIH guide for Care and Use of Laboratory Animals, federal and state regulations, and was approved by the Cornell University Institutional Animal Care and Use Committee (IACUC). Animals were brought into the research unit and given a 3-day acclimatization period prior to any procedure. Daily record logs of medical procedures were maintained. Rodent cages were replaced weekly. Animals were on a 12/12h light-dark cycle and allowed food and water *ad libitum*. Group housing prior to medical procedures provided socialization. ARRIVE guidelines for reporting *in vivo* experiments were used throughout (McGrath, Drummond, McLachlan, Kilkenny, & Wainwright, 2010).

Animal Surgeries

To determine the effects of NSECM on nerve regeneration in the mouse, the left sciatic nerves of male C57/BL/6J mice were transected proximal to the bifurcation and immediately repaired (figure 3). Mice were anesthetized with 3% isoflurane and maintained under anesthesia with 2% isoflurane and oxygen. Analgesia was provided by subcutaneous meloxicam (4mg/kg) injection pre-operatively and 24 hours after surgery. The sciatic nerve was exposed and transected. Proximal and distal nerve stumps were aligned and sutured 1mm into nerve conduits with 10-0

suture (Ethilon) to create a non-critical defect (3mm). Animals were divided into three groups and the conduit was filled with NSECM (15mg/mL, n=29), 0.7% agarose (n=29) or left unfilled (negative control, n=29). The agarose group was included to control for mechanical environment provided by NSECM hydrogel. Muscle and cutaneous layers were closed, as routinely performed.

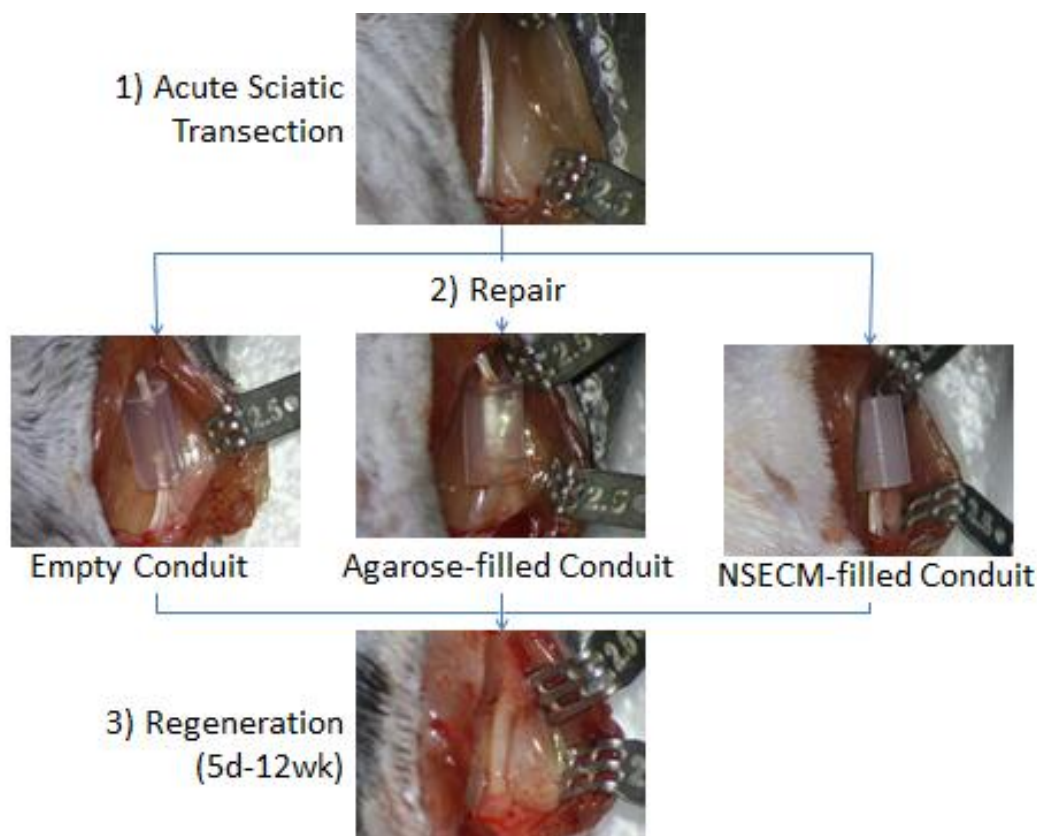


Figure 3: Surgical experimental groups. Acute sciatic transection followed by immediate repair with an inert silicone conduit left empty (control) or filled with 0.7% agarose or 15mg/mL NSECM.

Preparation of Surgical Implants and gels

Conduits were prepared by trimming an autoclave-sterilizing silicone tubing to 5mm length (Tuzic, Siliclear tubing, 1.98mm ID). Agarose (Seaprep, Rockland ME) was prepared by mixing 1.4% agarose solution in DI water then autoclaving to yield 0.7% agarose gel. Sterilized

conduits were filled with liquid agarose and incubated at 4°C for 15 minutes to allow gellation before surgical implantation. NSECM digestion products were stored in 1mL aliquots at 20mg/mL at -80°C. NSECM gel solution was prepared by adjusting the pH of the digestion products to 7.4 and diluting to 15mg/mL. Neutralization was accomplished by adding one-tenth of the digest volume of 0.1N NaOH and one-ninth of the digest volume of 10XPBS; dilution was accomplished using the appropriate volume of 1x DPBS. The neutralized gel solution was kept on ice prior to use. Conduits were either filled prior to surgery or immediately after surgical implantation. In the former case, sterilized conduits were filled with NSECM and placed on a heating pad for 20 minutes, and the pre-gelled conduits were implanted surgically. In the latter case, an empty conduit was surgically implanted and the NSECM was injected *in situ* and allowed to gel for 10 minutes at body temperature.

Mouse Sciatic Nerve Immunofluorescence for Macrophages (CCR7/CD68 and CD206/CD68)

To quantify spatial and temporal effects of NSECM on macrophages during nerve regeneration, immunohistochemistry was performed at 5 days after repair to identify macrophage populations. Mice (n=5/group) were euthanized with pentobarbital and the conduit and proximal and distal stumps were removed intact. The conduit and epineurial sutures were removed and the regenerated tissues and proximal and distal stumps were mounted on a slide and fixed in modified Zamboni's solution (paraformaldehyde, picric acid, phosphate buffer) overnight for immunofluorescent labeling as described below.

Samples were embedded in paraffin and sectioned at 4 µm on Probe-On microscope slides (Fischer Scientific) for immunofluorescent labeling to assess the host macrophage response. Macrophage M1 and M2 labels were used on consecutive slides from nerves harvested 5 days

after repair. Two slides were generated for each label; each slide contained two consecutive nerve sections. After deparaffinization and rehydration, antigen retrieval was performed by steaming slides for 20 min either in Tris EDTA buffer (pH 9) for macrophages labeling, followed by incubation for 30 min at room temperature. Sections were then processed with a MicroProbe System (Fisher Scientific) and phosphate buffered saline containing 0.05% Tween 20 (PBST) was used for washing between each of the steps described below.

To identify M2 macrophages (CD68+ and CD206+), the sections were first blocked with 10% donkey serum plus 2xcasein for 30 min at room temp. After that, the sections were incubated with primary antibodies mix of rabbit anti- CD68 (pan-macrophage, 1:50) and goat anti-CD206 (M2, 1:100) for 90 minutes at room temp and followed by overnight incubation at 4°C . Then, the slides were washed with PBST for 5min, twice, and incubated with: biotinylated donkey anti-goat IgG (1:200) for 30 minutes followed by streptavidin- Texas Red (1:200) for 20 minutes at room temperature to label M2 macrophages in red. After washing, the slides were further incubated with Alexa-Fluor488 donkey anti-rabbit (1:100) for 1 hour at room temperature to label pan-macrophages in green.

To identify M1 macrophages (CD68+CCR7+), the sections were first blocked with 10% goat serum plus 2xcasaein for 30 min at room temp. After that, the sections were incubated with rabbit anti-CD68 (pan-macrophage, 1:50) for 90 minutes at room temperature. Then, the sections were washed and then incubated with biotinylated goat anti-Rabbit (1:200) for 30 minutes followed by incubation with streptavidin-AlexaFluor488 (1:200) for 20 minutes at room temperature to label pan-macrophage in green. In order to co-label with M1 macrophages, the sections were subsequently incubated with normal rabbit IgG (1:100) and then goat anti-rabbit Fab fragment (1:50) for 60 minutes each at 37°C. After washing, the sections were incubated with rabbit anti-CCR7 (M1, 1:500) for 90 minutes at room temperature. Finally, the sections were incubated with Texas-red goat anti-rabbit (1:200) for 30 minutes at room temperature to

label M1 macrophages in red. Sections were washed and coverslipped with mounting media containing DAPI (Vectashield, Vector Laboratories).

For negative controls, the primary antibodies were replaced with species-specific isotype IgG at equivalent concentrations. Antibody host, isotype, dilution, and supplier information are provided in Table 3.

Slides were imaged using Aperio Scanscope fluorescent microscopy to obtain images at 40x magnification. Three high power fields were assessed in the proximal stump, regenerative bridge, and distal stump; for macrophage populations CD68+ CCR7+ were identified as M1 and CD68+ CD206+ were identified as M2. Positive macrophages were counted using ImageJ.

Table 3: Antibodies for Double Immunofluorescence

Antibody	Host	Isotype	Dilution	Supplier
CD68	Rabbit	IgG	50	Abcam
CD206	Goat	IgG	100	Santa Cruz
CCR7	Rabbit	IgG	500	Abcam
Streptavidin-AlexaFluor488		N/A	200	Abcam
TexasRed Goat anti-Rabbit	Goat	IgG	200	Abcam

Isolation of cell populations using fluorescence assisted cell sorting (FACS)

Mice were euthanized at 5, 14, or 28 days after repair to describe the early, mid, and late immune responses to nerve injury. The regenerative bridge was harvested within the conduit by transecting the proximal and distal sciatic nerve stumps 1mm from the end of the 5mm conduit. The epineurial sutures were cut and the regenerative bridge was removed from the conduit and placed in a petri dish with 1mL RPMI-1640 (Corning) and was cut into 1mm pieces. The tissues

were then transferred to a 50mL conical with 10mL of digestion buffer. Digestion buffer comprised of 3mg/mL collagenase type I (Sigma), 1mg/mL hyaluronidase (Sigma), and 0.5mL of 1mM HEPES in RPMI-1640. After 1hour digestion in a 37°C water bath, tissues were strained through a 70µm mesh strainer (BD Biosciences) to obtain a single cell suspension. The cells were centrifuged at 300g for 10 minutes and resuspended in 1mL red blood cell lysis buffer (eBioscience) for 10 minutes on ice. After lysis reaction, the solution was quenched with 5mL DPBS and centrifuged again at 300g for 10 minutes. The cell pellet was resuspended in 0.5% BSA (Sigma) in DPBS and cells were plated on a v-bottom 96-well plate (Nunc, Thermo Scientific) for FACS.

Cells were labeled for FACS for 45 minutes at 4°C using species-specific antibodies to label macrophages and other immune cells. See table 4 for antibodies and working dilutions. All wash steps were performed with 0.5% BSA in DPBS.

Table 4: Surface-stain Antibodies for FACS

Label	Dilution	Fluorochrome	Distributor	Host source	Specificity
Cd16/32	1:50	BV-605	Biolegend	Rat	Pan macrophage
F4/80	1:200	PE-Cy7	eBioscience	Rat	Pan macrophage
Cd11b	1:200	Pacific Blue	eBioscience	Rat	Pan macrophage
Cd14	1:100	PE-Cy7	BioLegend	Rat	Pan macrophage
Ly6G	1:100	APC	BioLegend	Rat	Granulocytes
Siglec F	1:64	APC	Miltenyi Biotec	Rat	Eosinophils
CD19	1:400	APC	eBioscience	Rat	B Lymphocytes
CD3e	1:80	APC	eBioscience	Armenian Hamster	T Lymphocytes
PI	1:200		BD Bioscience		Viability

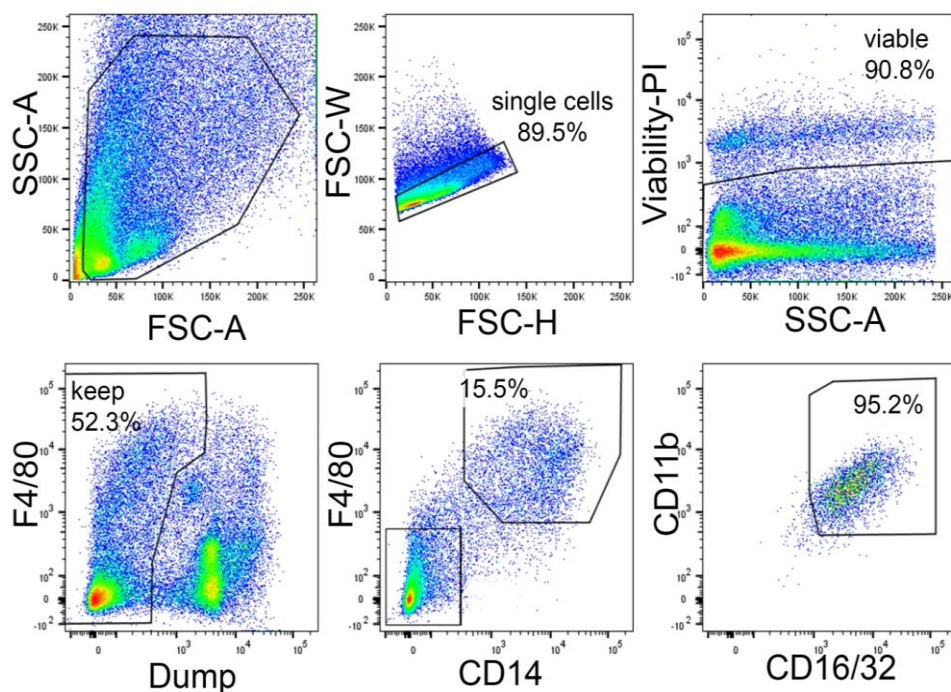


Figure 4: Sorting strategy for macrophage isolation. Macrophages were identified as F4/80+, CD14+, CD16/32+ and CD11b+

Cells were analyzed and sorted using fluorescence activated cell sorter FACSriaIII (BD Biosciences) using FACSDiva software (BD Biosciences version 6.1.3). The fluorochromes were excited with the instrument's 405nm, 488nm, 532nm, and 633nm lasers. The appropriate detection filters were used (Table 2). Compensation beads (OneComp, eBioscience) were used to set the compensation matrix. Fluorescence was determined by gating against appropriate controls (unstained, fluorescence minus one) on samples prepared in parallel. Gates were set such that less than 1% of positive events were recorded when acquiring the corresponding negative control. Figure 4, above, shows the gating strategy used. Cells were gated on forward and side scatter area for general cell size, forward scatter height and width to exclude doublets, side scatter and propidium iodide (PI) to exclude dead cells, and F4/80 versus APC to remove cells in the dump channel (APC). Macrophages were defined as all viable single cells that were

PI⁻Dump⁻F4/80⁺CD14⁺. Inflammatory macrophages can have reduced F4/80 expression, so if the macrophage population was close to or crossed the lower limit of the gate, coexpression of CD11b and CD16/32 were used to adjust the macrophage gate. To assure specificity, purity checks were performed by re-analyzing a subset of sorted cells and only sorts with >80% enrichment were accepted. Prior to sorting, the nozzle, sheath, and sample lines were washed with RNase Away (Ambion) for 15 minutes then flushed with preservative-free sheath solution (Biosure) for 2-3 minutes to remove RNases. A 100µm ceramic nozzle (BD Biosciences), sheath pressure of 20psi, flow rate < 3 and acquisition rate of <3000 events per second were used as conditions optimized for neuronal cell sorting as previously described (Pruszek, Ludwig, Blak, Alavian, & Isacson, 2012). Macrophages were sorted into 0.5% BSA in DPBS in RNase-free, lo-bind eppendorf tubes (Zymogen). Sorted cells were lysed with 1µL/4000 cells (minimum 5µL) of a 1:1 solution of RNA lysis buffer (Qiagen) in RNase-free water and stored at -80°C until processed for gene expression analysis. Data was analyzed using FlowJo software (TreeStar). Quantification of gene expression was performed as described above using NanoString Technologies.

Motor Neuron Regeneration

Motor neuron regeneration was evaluated via retrograde labeling to quantify regeneration across the length of the silicone conduit using RetroDISCO (Zygelyte *et al* 2015, in review). Mice were allowed to recover for 2, 4, or 8 weeks after repair, and were anesthetized. The nerve, distal to the site of repair, was approached surgically. The sutures and conduit around the nerve were removed and the nerve was transected distal to the original transection site. The proximal nerve stump was immersed in a well filled with retrograde tracer, 10% FluoroRuby (LifeSciences) in 2% DMSO. The top of the well was sealed with Vaseline and the nerve was allowed to soak for 1 hour (Al-Majed, Neumann, Brushart, & Gordon, 2000; Midha *et al.*, 2005).

Animals were allowed to recover for five days to allow retrograde transport of the tracer and fluorescent labeling of the cell bodies.

Spinal cord harvest

Five days after labeling, mice were anaesthetized and perfused with 20mL chilled saline followed by 30mL 4% paraformaldehyde (Sigma) (Midha et al., 2005, Al-Majed et al., 2000). Following perfusion, intact spinal cords from the cervical spine to the conus medullaris were collected to ensure the entire L4-S3 spinal segments containing the sciatic motor neuron cell body pool was harvested. Explanted cords were fixed in 4% paraformaldehyde overnight.

Optical clearing was achieved as described previously [Zygelyte *et al* 2015, in review]. Briefly, explanted spinal cords were dehydrated by immersion in increasing concentrations of tetrahydrofuran (THF, Sigma Aldrich) solutions (50-80%), then immersed three times in 100% THF, each for 30 minutes. Spines were then immersed in 100% dichloromethane (DCM, Sigma Aldrich) for lipid extraction for 25 minutes. Optical clearing was achieved by immersing the spines for 30 minutes in 100% benzyl ether (DBE, Sigma-Aldrich), which has the same refractive index of the remaining proteins. Following clearing, spinal cords were mounted with the dorsal side down on Superfrost® Plus microscope slides (Fisher) with FastWell™ reagent barriers (Grace Bio-Labs) immersed in DBE, and sealed with a glass coverslip. Throughout this process, the spinal cords were protected from UV light exposure to prevent degradation of the fluorescent signal.

This method improves accuracy in quantification of motor neuron regeneration over previously used methods. Retrograde tracing is recommended over axon counts, as axonal sprouting can confound determination of regenerative success (Wood, Kemp, Weber, Borschel, & Gordon, 2011). Further, clearing and imaging the whole spinal cord over standard cryosectioning decreases variability in loss of tissue and in double-counting cells split between sections.

Imaging

Spinal cords mounted in DBE were imaged at 10x magnification with 6.4 μ m z-stacks using a confocal microscope (Zeiss 510, Thornwood, NY; 561nm for FluoroRuby). The confocal microscope was set at a bit depth of 12, averaging of 2, laser intensity 8, 1.0 airy units pinhole, and 400-600 gain. Adjustments were made to the gain as needed to obtain a bright image.

Image J software (NIH) was used to identify and manually count cell bodies (Figure 5).

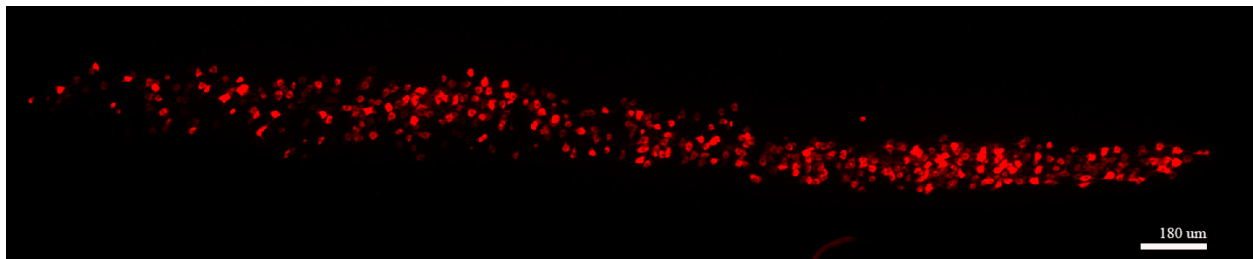


Figure 5: Retrograde-labeled motor neurons from a mouse 4 weeks after nerve repair.

Data analysis

Continuous outcome measures were assessed using t-test or ANOVA with Tukey's post hoc tests. All data were analyzed using JMP 10 (SAS Institute Inc., Cary, NC). Significance was set as $p < 0.05$ throughout.

Gene expression analysis:

Nanostring nSolver Analysis Software (NanoString Technologies) was used to normalize raw gene expression data. First, raw data were generated; total RNA transcript counts per sample were calculated and negative controls were used to determine background.

Next, expression was normalized against housekeeping genes (ACTb, ANKRD27, GAPDH, HMBS, HPRT, RICTOR, and TBP). Three housekeeping genes with expression above background and variation below 30% were chosen for normalization. A normalization factor was

calculated and applied for each sample to correct for process or system (nonbiological) variation and allow comparison between all samples. Samples that were flagged for quality control or normalization errors due to average expression below background were excluded. These were due to insufficient RNA quantity or poor quality, primarily due to nuclease activity.

Normalized data were then analyzed using JMP software (SAS). Genes with average expression across all samples below background were considered as not expressed in these genes and were excluded. Hierarchical clustering and principal component analysis were performed to visualize expression patterns between groups.

For each gene, a mixed effect for response screening was used to determine genes with variation in normalized expression across groups while controlling for false discovery rate (FDR, $p \leq 0.05$). For genes meeting this FDR cutoff, mixed effect models were used to determine variation between *in vitro* stimulant and the interaction between group (NSECM, agarose, control) and time (5, 14, and 28 days) for *in vivo* data. Dunnett's test was used for comparisons of BMDM data against M0 control. Tukey's post hoc test for multiple comparisons was used to compare the differences in mean gene expression between *in vivo* sorted samples.

Gene expression data were represented graphically using GraphPad Prism as the mean plus standard deviation of mRNA count for each replicate in the group.

RESULTS

Bone Marrow Derived Macrophage Culture

Flow cytometry data for cell surface and intracellular markers on bone marrow derived macrophages demonstrated that, as anticipated, M2 (IL4) macrophages had significantly higher expression of Arg1 than unstimulated (M0) macrophages). M1 (IFNg/LPS) stimulation was associated with a mild increase in Arg1. In contrast, NSECM stimulated macrophages demonstrated reduced Arg1 expression (Figure 6). To further evaluate the NSECM-stimulated cells in comparison to known extremes of macrophage polarization, gene expression analysis was also performed.

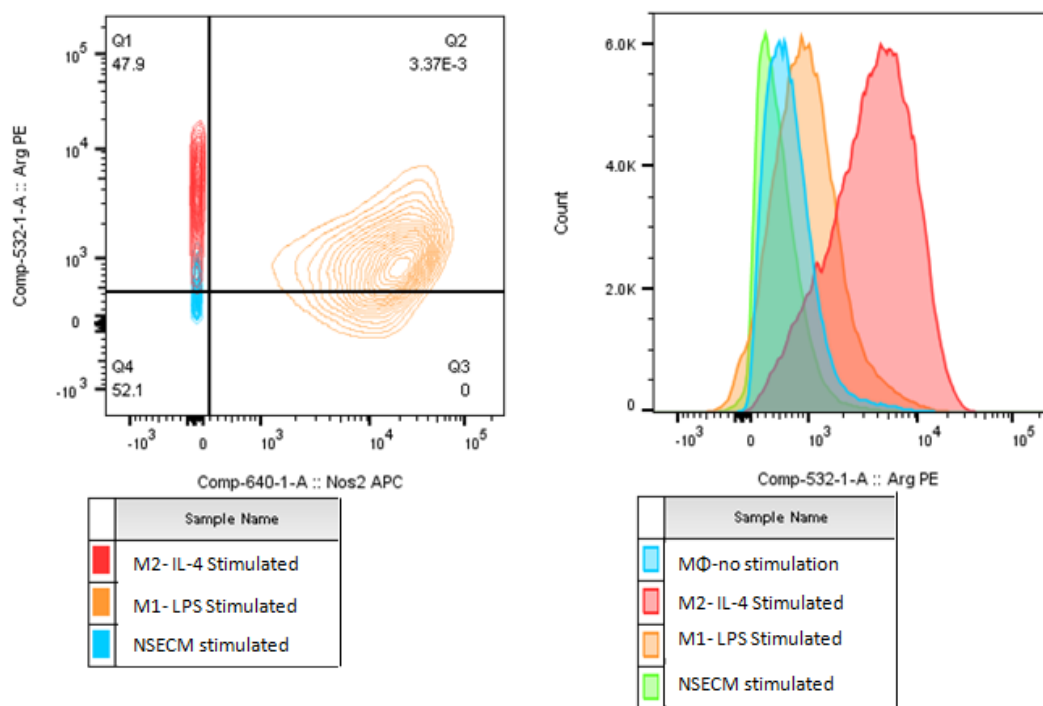


Figure 6: Flow cytometric analysis of cultured macrophages using Arg1 and iNOS2 markers. The figure on the left compares Arg1 and iNOS expression on M1, M2, and NSECM-stimulated macrophages. The figure on the right shows a histogram of Arg1 fluorescence for M0, M1, M2, and NSECM-stimulated macrophages.

To explore the effects of NSECM on macrophage phenotype, gene expression analysis was performed using a NanoString panel of 90 genes related to macrophage phenotype and function. Sample counts were normalized using housekeeping genes, allowing comparisons across multiple samples. Normalized and averaged gene expression mRNA counts for all genes are shown in table 5. Genes with average expression below background were not included in analyses. Genes that had a significant difference between groups after correction for false discovery rate (FDR) are shown in figure 7.

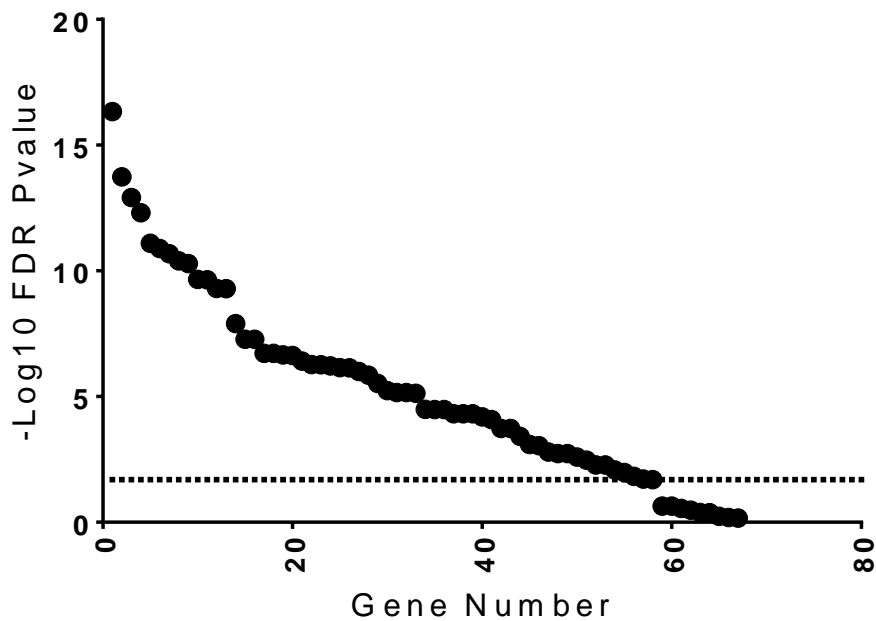


Figure 7: $-\log_{10}(\text{FDR p-values})$ ranked for each gene analyzed in cultured macrophage samples. Genes above the threshold line are $\text{FDR p-value} < 0.05$

Table 5: Normalized gene expression and p-values for bone-marrow derived macrophages

Gene	M0	M1	M2	NSECM	FDR-Pvalue
Chemokine					
Ccl11	6.30	19.33	7.66	5.07	nd
Ccl17	11.47	15.41	159.71	11.11	7.48E-06
Ccl2	20118.33	3741.61	21088.00	13632.05	1.86E-04
Ccl22	60.23	2977.30	559.77	44.51	1.83E-14
Ccl24	418.98	25.24	2043.96	85.52	4.90E-05
Ccl5	596.69	231016.86	339.91	515.16	5.41E-07
Cxcl10	2115.64	9240.12	242.75	657.88	1.29E-11
Cxcl11	29.84	1124.89	27.88	19.30	4.94E-13
Cxcl13	10.55	29.24	38.89	10.28	3.42E-03
Cxcl16	3261.33	9510.87	1823.10	2915.76	3.28E-05
Cxcl4	2869.44	86.62	1172.12	3401.63	3.28E-05
Cxcl9	7.36	9107.16	6.04	4.79	5.25E-08
Cytokine					
Ccl1	10.61	28.53	12.72	6.29	nd
Ccl20	4.96	20.68	7.18	3.15	nd
lfn3	11.42	32.78	27.01	12.87	nd
Il10	438.31	32.48	216.57	356.11	1.06E-02
Il12	389.67	84636.18	47.21	73.70	1.41E-06
Il17a	18.81	37.89	21.75	14.12	5.25E-03
Il1a	4585.93	2562.84	3853.74	2957.30	6.49E-01
Il1b	24523.05	42904.46	12886.15	11144.15	4.90E-05
Il2	10.50	20.51	16.06	8.36	nd
Il22	9.80	149.81	8.76	8.38	1.86E-04
Il23p19	116.64	41.93	182.57	59.57	2.30E-01
Il27	44.13	723.49	32.29	36.79	2.21E-07
Il6	259.44	29576.48	1618.08	133.95	4.63E-17
Lif	379.92	184.20	392.37	201.17	3.31E-01
tgfb	3428.32	693.56	4263.26	3427.12	1.25E-08
Tnf	20458.36	1527.20	10084.08	16429.41	1.87E-03
Cytokine Regulator					
Socs1	70.25	1071.61	199.66	80.74	2.10E-11
Socs2	41.94	50.46	292.92	20.35	5.25E-08
Socs3	1531.09	576.95	1140.22	922.89	2.02E-02
Enzyme					
Alox15	15.54	31.91	13.03	9.56	nd
Arg1	31.60	627.97	50815.13	97.69	2.27E-10
Chi3l3 Ym1	222.99	32.35	33218.30	167.94	4.90E-05

Gene	M0	M1	M2	NSECM	FDR-Pvalue
Nos2	15.43	27118.96	23.34	20.14	5.40E-07
tgm2	3639.32	3405.41	4593.62	2533.26	1.92E-02
Growth Factor					
BDNF	7.19	17.08	10.02	6.07	nd
CNTF	45.84	33.70	64.82	36.17	2.80E-01
Egf	5.39	19.59	6.94	4.65	nd
FGF1	27.78	25.18	8.63	14.37	nd
FGF2	22.59	28.30	28.50	20.23	nd
Gdnf	51.88	57.90	83.57	47.59	5.86E-01
Hgf	441.37	35.80	245.90	261.66	8.95E-04
IGF1	1981.95	34.93	4997.16	2528.03	5.15E-10
IGF2	15.01	21.13	19.86	13.28	nd
Ngf	15.31	23.86	12.82	11.80	nd
Ntf3	5.89	17.15	9.29	4.68	nd
Ntf5	8.92	24.73	6.57	4.86	nd
Pdgfb	536.99	241.30	619.67	1395.41	1.61E-03
VEGFA	3518.97	4211.43	2743.36	2840.37	6.88E-01
Receptor					
Ccr2	1491.36	132.15	1338.95	447.69	5.31E-03
CCR7	22.89	14289.06	153.33	18.13	1.92E-07
CD163	72.41	20.08	60.98	31.66	8.14E-04
CD206	1973.60	20.55	9577.45	1092.37	2.33E-07
CD40	1016.91	10706.47	1283.73	575.39	4.04E-11
Cd80	317.24	1776.94	327.66	221.43	7.99E-12
CD86	632.62	2244.73	546.96	424.61	5.82E-06
Il1ra Il1rn	2680.86	4775.79	4074.84	3373.42	2.30E-01
Il4ra	1449.27	2454.26	1088.11	1209.84	3.05E-06
Mac1	3180.59	1062.31	2034.37	3320.57	1.87E-03
Mac2	266.24	109.81	749.72	794.68	3.25E-05
Marco	265.67	21507.80	131.97	1537.73	6.47E-05
NGR	8.45	33.84	10.03	8.91	nd
p75NTR	11.38	48.91	8.12	7.99	6.93E-06
SRAI	5448.94	1556.81	4401.74	5271.38	1.02E-06
SRAII	2714.44	24.37	2064.45	873.48	6.90E-06
Tlr1	479.94	670.62	487.95	257.77	7.27E-07
Tlr2	3834.54	102.80	1419.23	1759.65	8.32E-05
Tlr4	1359.59	214.32	2040.24	1048.84	2.21E-10
Tlr8	2970.37	562.62	4546.59	2061.00	7.17E-07
Secreted Protein					
Retnla Fizz1	16.44	35.01	284296.07	16.86	2.58E-03
Transcription Factor					

Gene	M0	M1	M2	NSECM	FDR-Pvalue
lrf3	372.71	223.28	319.15	298.54	8.36E-03
lrf4	59.09	37.08	635.14	66.59	5.16E-11
lrf5	2830.07	2652.83	3718.61	2456.16	1.49E-02
Nfil3	928.77	2276.09	2753.16	587.72	6.09E-07
Nfkbiz	9470.86	1326.08	4363.84	5100.65	3.88E-04
PPARg	76.94	20.35	264.42	116.10	3.89E-07
Sbno2	440.27	482.99	469.57	408.37	4.15E-01
Stat1	665.28	4005.66	485.01	524.59	5.04E-10
Stat2	137.27	1708.14	131.44	106.52	1.21E-13
Stat3	1539.38	3356.53	1489.25	1160.54	1.92E-07
Stat6	2414.36	2074.76	2133.80	2081.11	4.09E-01

First, hierarchical clustering and principle component analysis were performed to evaluate broad distinctions between stimulation groups. Based on normalized gene expression data, M1 macrophages were the most distinct outgroup, followed by the M2 macrophages, then M0 macrophages (figure 8).

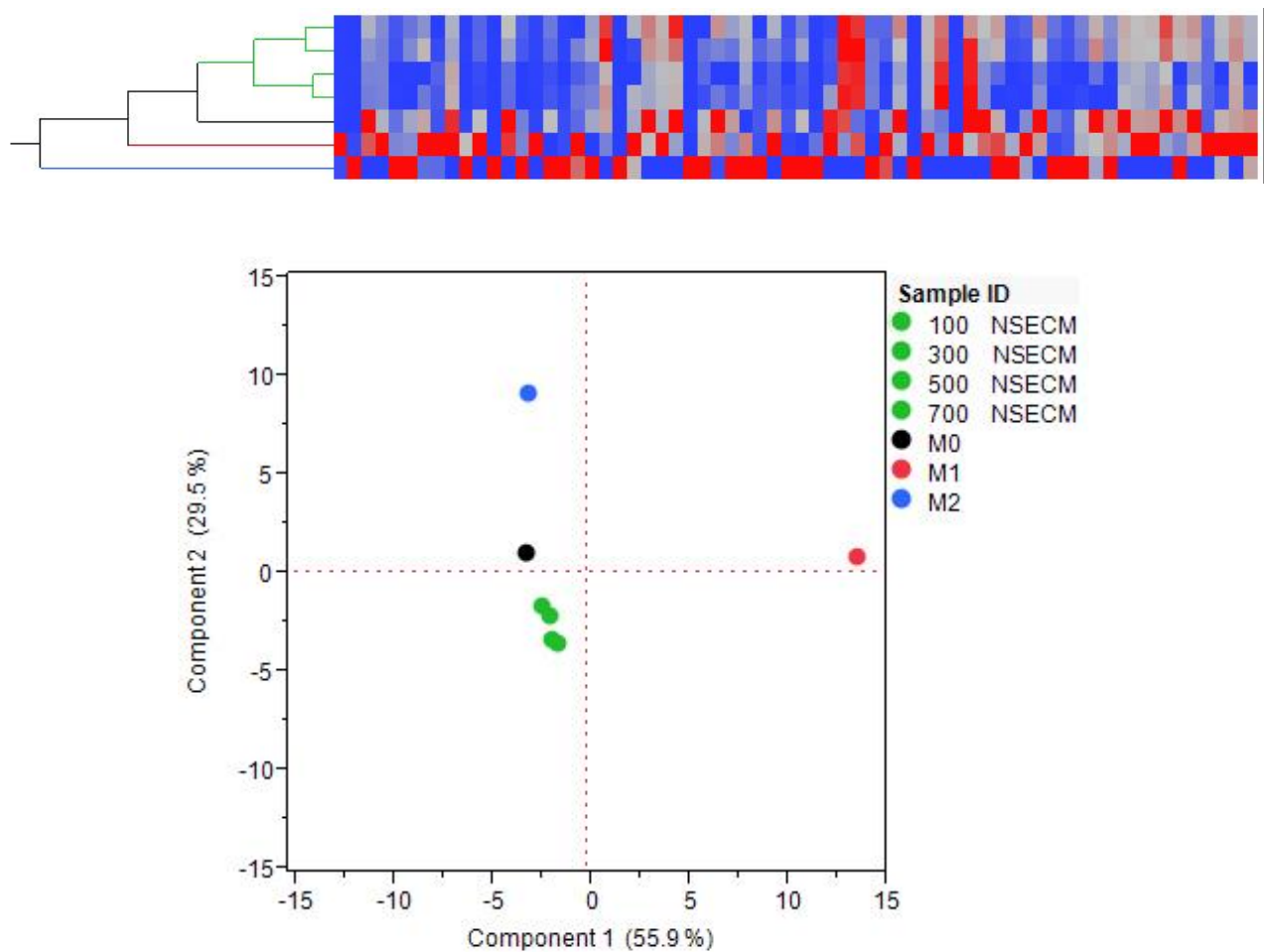


Figure 8: Hierarchical clustering and principal component analysis of bone marrow-derived macrophage gene expression data. Data show distinct clustering of macrophages with extreme polarization (M1-IFN γ /LPS) and M2 (IL4). The gene expression profile of macrophages stimulated with NSECM is distinct from but most similar to unstimulated macrophages (M0).

NSECM-stimulated macrophages clustered independently and were most similar to M0 macrophages. PCA reiterates what the heat map cluster suggests about group similarity. M1 cells map the furthest away in a distinct quadrant. M2 cells map nearly oppositely from M1 cells. NSECM-stimulated cells are in a distinct cluster relative to these two control phenotypes, and they map closest to M0 cells. M0 cells map in between NSECM and M2 cells, again suggesting that NSECM-stimulated cells are highly distinct from the M2 phenotype.

To further evaluate differences between NSECM-stimulated and control cells, genes meeting a FDR cut off of $p < 0.05$ were evaluated relative to M0. No significant differences in macrophage gene expression between different NSECM concentrations were observed, so these results were pooled to a single NSECM group for individual gene expression analyses.

For most genes, significance in expression mRNA counts was due to the extreme expression profiles produced in the M1 (IFN γ /LPS) and M2 (IL4) groups.

Compared to M0 macrophages, IL-4 stimulated M2 macrophages were found to have increased expression of genes encoding enzymes *Arg1* and *Chi3l3*; receptors *CD206*, *MAC2*, *TLR2*, *TLR4*, *TLR8*, chemokines *CCL17*, *CCL22*, *CCL24*, *CXCL10*, *CXCL13*; growth factors *HGF*, *IGF1*, and *TGF β* ; secreted protein *RETNLA FIZZ1*; transcription factors and regulators *IRF4*, *NFIL3*, *NFKBIZ*, and *PPAR γ* ; and signaling regulator *SOCS2* (table 5). Additionally, M2 cells were found to have a decrease in *CXCL4* expression (appendix figure 18).

There was much variation in LPS and IFN γ -stimulated M1 cells, relative to M0 cells. We found decreased expression of genes encoding chemokines *CCL2*, *CXCL4*; cytokines *IL10*, and *TNF*; signaling regulator *SOCS3*; growth factors *TGF β* , *HGF*, and *IGF1*; enzyme *NOS2*; membrane receptors *CCR2*, *CD163*, *MAC1*, *SRAI*, *SRAII*, *TLR2*, *TLR4*, and *TLR8*; transcription factor *IRF3*; and transcription regulator *NFKBIZ*. In addition, we found increased expression of chemokines *CCL22*, *CCL5*, *CXCL10*, *CXCL11*, *CXCL16*, *CXCL9*; cytokines *IL12*, *IL17 α* , *IL1 β* ,

IL22, IL27, IL6, signaling regulator *SOCS1*; receptors *CCR7, CD40, CD80, CD86, IL4 α , p75NTR, MARCO, TLR1*; transcription factors *NFIL3, STAT1, STAT2, and STAT3* (appendix figures 19 and 20) .

NSECM promoted a distinct gene expression pattern (figure 9). NSECM-stimulated cells were found to have decreased expression of genes encoding chemokines *CCL2* and *CXCL10*; signaling regulator *SOCS3*; growth factor *HGF*; receptors *CCR2, CD163, SRAII, TLR1, TLR2, TLR4*, and *TLR8*; transcription factor *IRF3*; and transcription regulator *NFKBIZ*.

NSECM-stimulated cells were also found to have increased expression of genes encoding angiogenesis-related growth factor *PDGFb* and receptor *MAC2*. Of these genes, decreased expression relative to M0 of *CD163, CCL2, CCR2, HGF, NFKBIZ, SRAII, SOCS3, TLR2, TLR4, TLR8*, and *IRF3* were in common with the expression pattern seen in M1 cells. In common with the expression pattern of M2 cells is the decrease in *CXCL10, HGF, NFKBIZ, TLR2*, and the increase seen in *MAC2*. Unique to NSECM was an increase in *PDGFb* expression and decrease in *IL1 β* and *TLR1* expression.

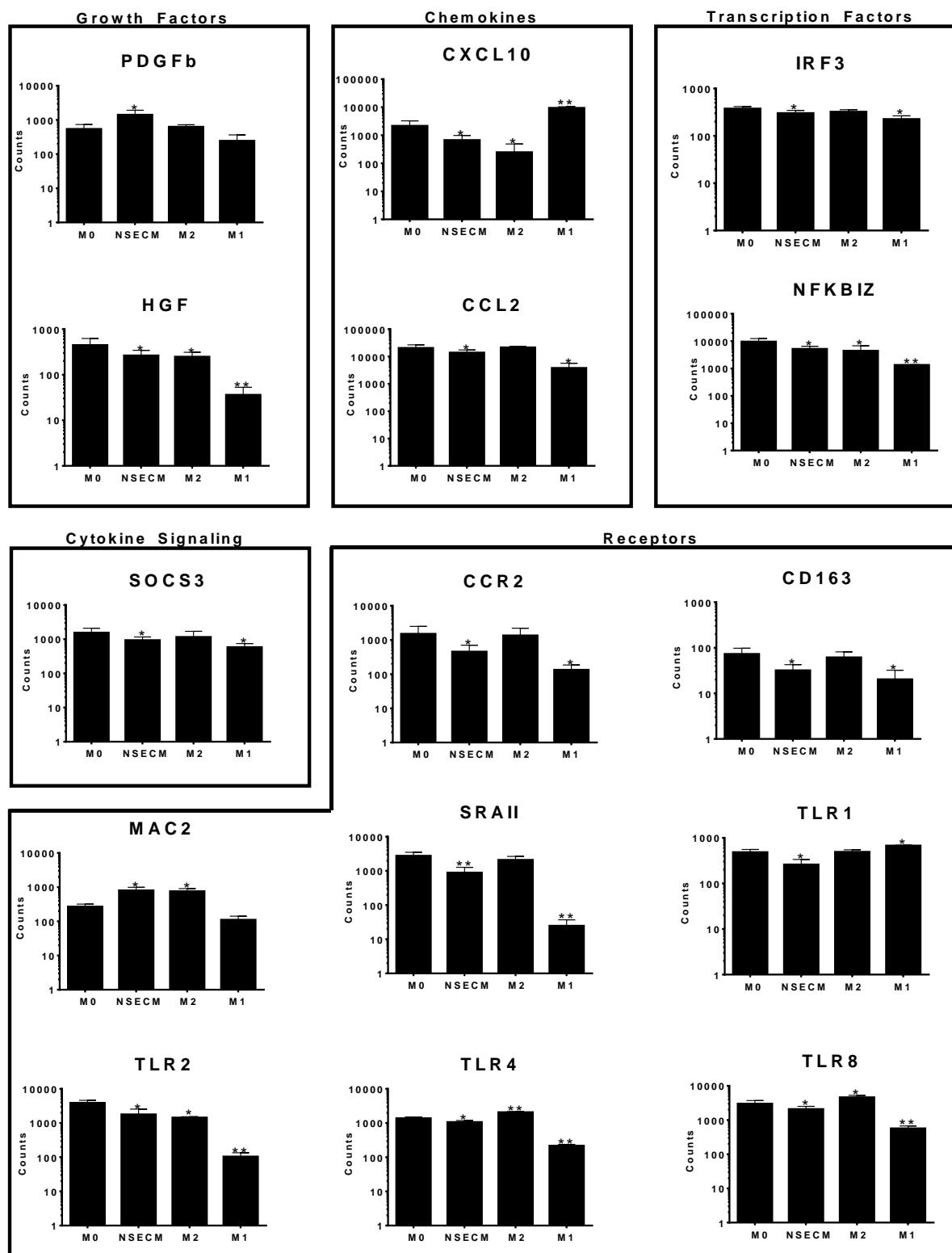


Figure 9: Gene expression (mRNA counts) in M1, M2, and NSECM-stimulated macrophages compared to M0. * $p < 0.05$, ** $p < 0.0001$.

Macrophage Immunohistochemistry

After evaluating the effects of NSECM on cultured cells compared to established phenotypic models, we evaluated the effects of NSECM *in vivo*. To evaluate the effects of NSECM on the migration and distribution of M1 and M2 macrophages, the regenerated sciatic tissues within NSECM-filled or empty conduits were harvested 5 days after injury and immunostained for M1(CCR7+/CD68+) or M2 (CD206+/CD68+) macrophages (figure 10). Two high power fields were taken in the proximal regenerative bridge, adjacent to the distal-most portion of the proximal nerve stump. Nerve sections from empty conduits had more M1 (CCR7+/CD68+) cells (average 130.5, S.D. 56.4), compared to nerve sections from NSECM-filled conduits (average 54, S.D. 66.5) (figure 10A below, $p < 0.05$, Tukey's post hoc test). There was no difference in M2 (CD206+/CD68+) cells in empty (average 108.6, S.D. 50.1) compared to NSECM-filled (figure 10B below, average 64.7, S.D. 103.2) conduits.

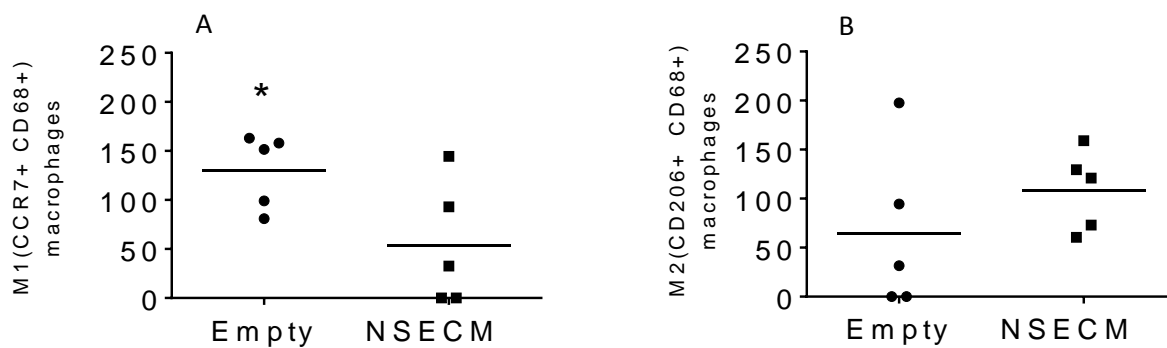


Figure 10: Immunohistochemical analyses of M1 and M2 macrophage populations in nerve tissue from empty and NSECM-filled conduits. A) M1 (CCR7+/CD68+) macrophages in left and right proximal hpf of the regenerative bridge. B) M2 (CD206+/CD68+) macrophages in left and right proximal hpf of the regenerative bridge.

Macrophage Sorting

Macrophage populations were then isolated from regenerated nerve tissue using fluorescence assisted cells sorting (FACS). Using FACSDiva software to quantify and sort cell populations, we found that macrophage populations increased slightly at day 14, with F4.80+/CD14+/CD11b+/CD16.32+ cells accounting for an average across groups of 32.5% (S.D. 7.4%) of all single, viable cells isolated from the regenerated tissues (figure 11). At day 5, F4.80+/CD14+/CD11b+/CD16.32+ cells accounted for 24.5% (S.D. 6.0%) of all single, viable cells. By day 28, populations started to decrease, with an average of 15.9% (S.D. 10.0%) F4.80+/CD14+/CD11b+/CD16.32+ cells accounting for all single, viable cells isolated from the regenerated tissues. There were no differences in macrophage numbers between experimental groups at these times.

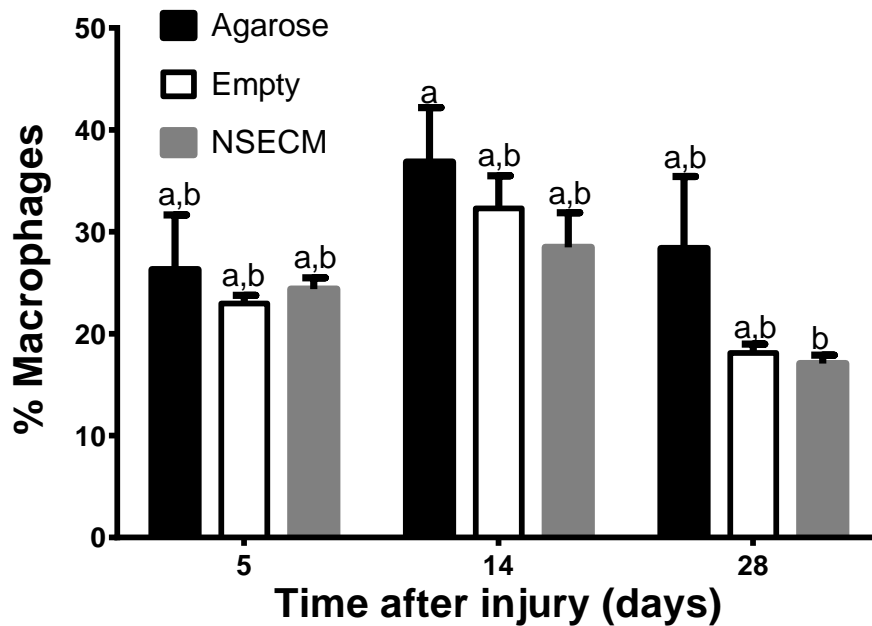


Figure 11: Proportion of macrophages sorted from total viable cells over time. Groups not connected by a letter are significantly different ($p < 0.05$, Tukey's post hoc test).

In Vivo Macrophage Gene Expression Analysis

Gene expression was then determined in sorted macrophage populations. Limited gene expression analyses have been performed to determine if the *in vitro* phenotype classification system matches *in vivo* populations; prior work has focused on a limited number of cell markers that define the dichotomous extremes of macrophage activation states. Our *in vivo* gene expression analysis study was performed to investigate the heterogeneity of macrophage populations over time during nerve regeneration and differences in gene expression after immunomodulation using NSECM. Gene expression was analyzed at days 5, 14, and 28 after sciatic injury and repair with empty (control), agarose, and NSECM conduits. Normalized and averaged gene expression mRNA counts for all genes can be found in appendix table 6. FDR-corrected p-values can be found in figure 12.

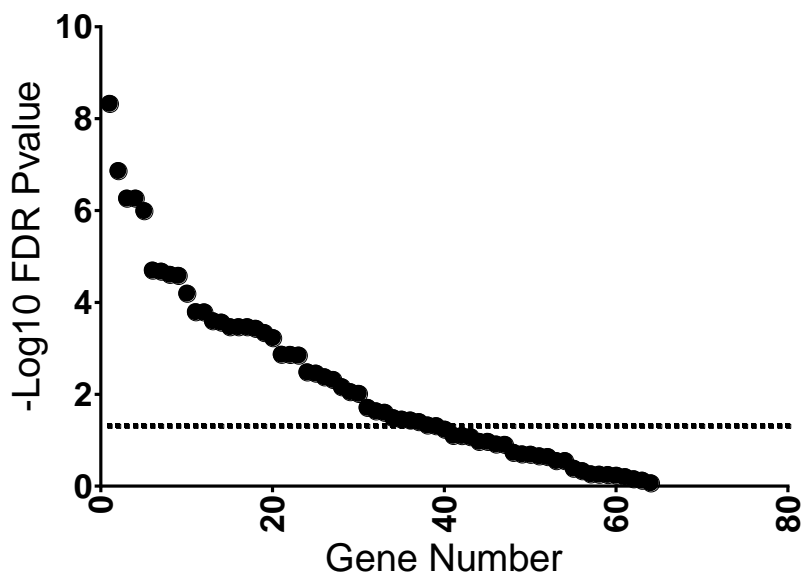


Figure 12: $-\text{Log}_{10}(\text{FDR p-values})$ ranked for each gene analyzed in macrophages sorted from injured nerves. Genes above the threshold line are FDR p-value < 0.05

First, hierarchical clustering and principle component analysis were performed to evaluate broad changes over time and between agarose, NSECM and empty conduit groups (figure 13). All groups (agarose, empty, NSECM) at the early time point (day 5) were clustered together and were distinct from groups at later time points. Empty and NSECM groups at day 14 cluster; then empty and NSECM at day 28; followed by agarose at day 14 and 28 clustering. These results suggest that the time point at which macrophages were evaluated may influence gene expression more strongly than any of the experimental groups used in this study. PCA confirmed the results suggested by hierarchical clustering. Agarose at day 14 was the most distinct cluster. Day 5 groups are also clustered very distinctly. Empty and NSECM groups at days 14 and 28 are broadly similar, existing closely within the same principal component quadrant. These observations were reflected in the analyses of individual gene expression.

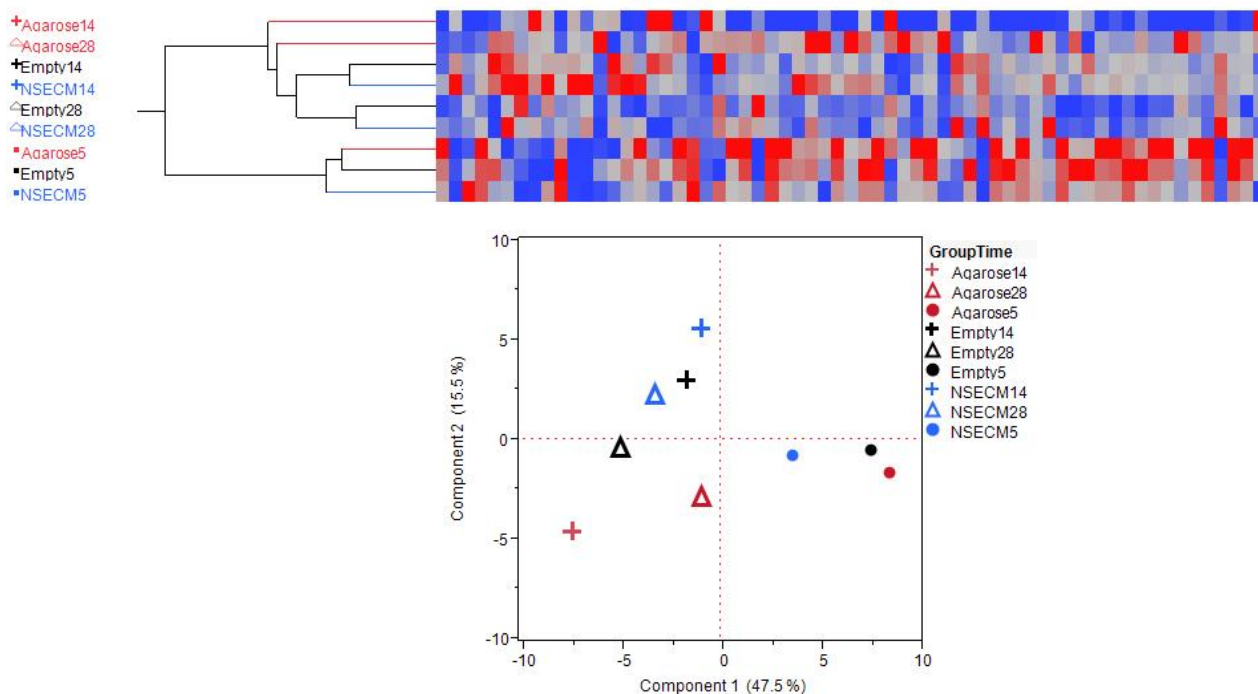


Figure 13: Hierarchical clustering and principal component analysis of gene expression profiles of macrophages isolated from regenerating nerves 5, 14, and 28 days after injury. Data show distinct clustering of expression of macrophages isolated at the earliest time point.

We found that M2 genes tended to decrease over time after injury and M1 genes tend to increase over time (figure 14). Between days 5 and 28, M2 genes encoding *Arg1*, *CD206*, *Chi3l3*, *IL4ra*, *STAT6* and *IL10* decreased, but *Retnla* *Fizz1* increased. Over the same time, M1 associated genes encoding *IL6* and *TNF* increased, but *IL1a* decreased. The M1 genes *CCR7* and *CXCL9* showed a transient increase at day 14, but no net change over the time periods evaluated, and both *CD80* and *iNos2* expression did not change over time. Notably, several M1 markers such as *IFNy*, *IL1β*, *IL12*, and *IL17a*, were not detected above background mRNA count. These changes tended to be more pronounced in macrophages from conduits filled with agarose, which showed increased expression of typically M2 associated genes (*Arg1*, *CD206*, *Chi3l3*) at early time points but lower expression of these genes relative to other groups at later time points. Conversely, agarose was associated with increased expression of M1 associated genes (*Nos2*, *TNF* and *IL6*) at later time points.

Figure 15 shows that immune mediators *CCL2*, *STAT2*, and *IRF5* decreased over time, but *CCL5* increased. *IL-6* and *STAT1* showed no changes over time. Negative regulators of inflammation *TLR8*, *IRF3*, and *STAT6* also decreased over time, but *SOCS1* and *IRF4* increased. *NFKBIZ* showed a transient decrease in expression at day 14, but overall no net change over the times evaluated. No significant changes were observed between experimental groups.

Next, we evaluated the expression of growth factors, cytokines, and chemokines (figure 16). *TGFβ* and *VEGF-A* expression tended to show high early expression with a decrease by 14 days. No significant changes in growth factor expression were observed between experimental groups. Chemokines *CCL11* and *CCL22* both had transient increases at day 14, but no net changes. Notably, *CCL11* expression was barely detectable above background mRNA count. *CCL24* increased over time, *CXCL16* decreased over time, and cytokine *IL27* showed no changes over time. NSECM treated macrophages did not show significant changes in

expression over time for chemokines *CCL5*, *CCL2*, *CXCL9*, and *CXCL16*, but did show increase expression of *CCL24* over time. Empty conduit groups tended to follow the same trends as NSECM. Similarly, cytokine expression (*IL10*, *IL1 α* , *IL27*, *IL6*, *TNF*) was maintained in empty and NSECM groups over time in contrast to agarose groups.

Lastly, we evaluated a variety of receptors, transcription factors, and signaling regulators, all of which largely decreased expression over time (appendix figure 21). Receptors *SRAI*, *TLR1*, *TLR2*, *TLR4*, and *MAC1* decreased over time, while *MAC2* had no change and *CCR2* transiently increased at day 14. Transcription factors *NFIL3*, *SBNO2*, *STAT3*, and cytokine regulator *SOCS3* all decreased over time as well.

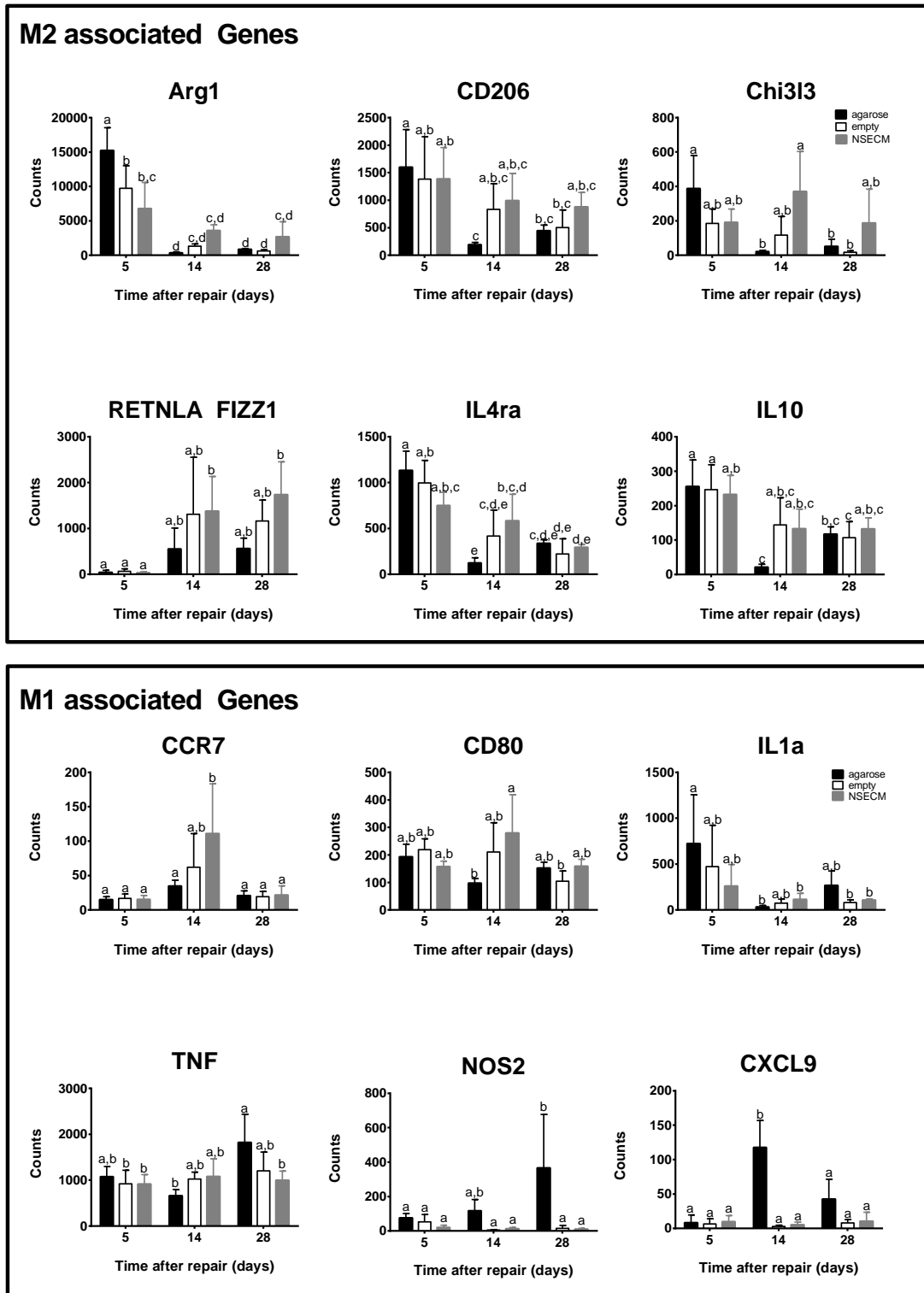


Figure 14: M2- and M1- associated gene expression from macrophages isolated from the site of nerve injury and repair. Groups not connected by the same letter are significantly different ($p < 0.05$, Tukey's post hoc test).

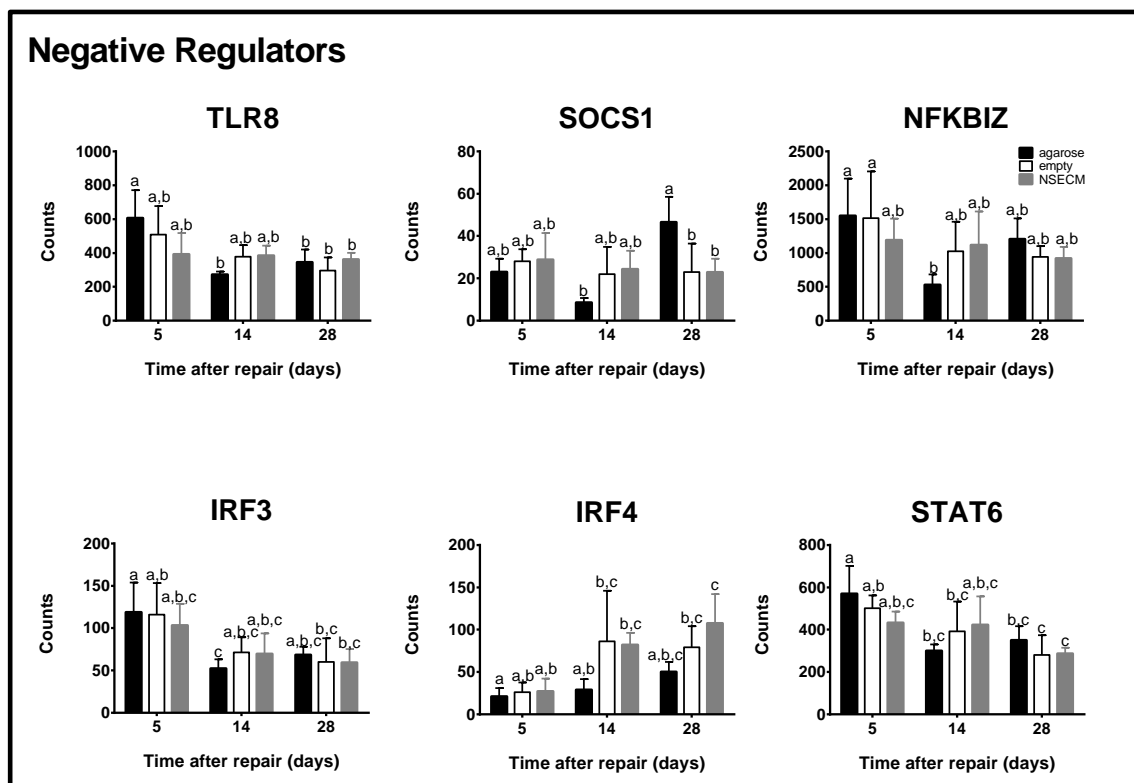
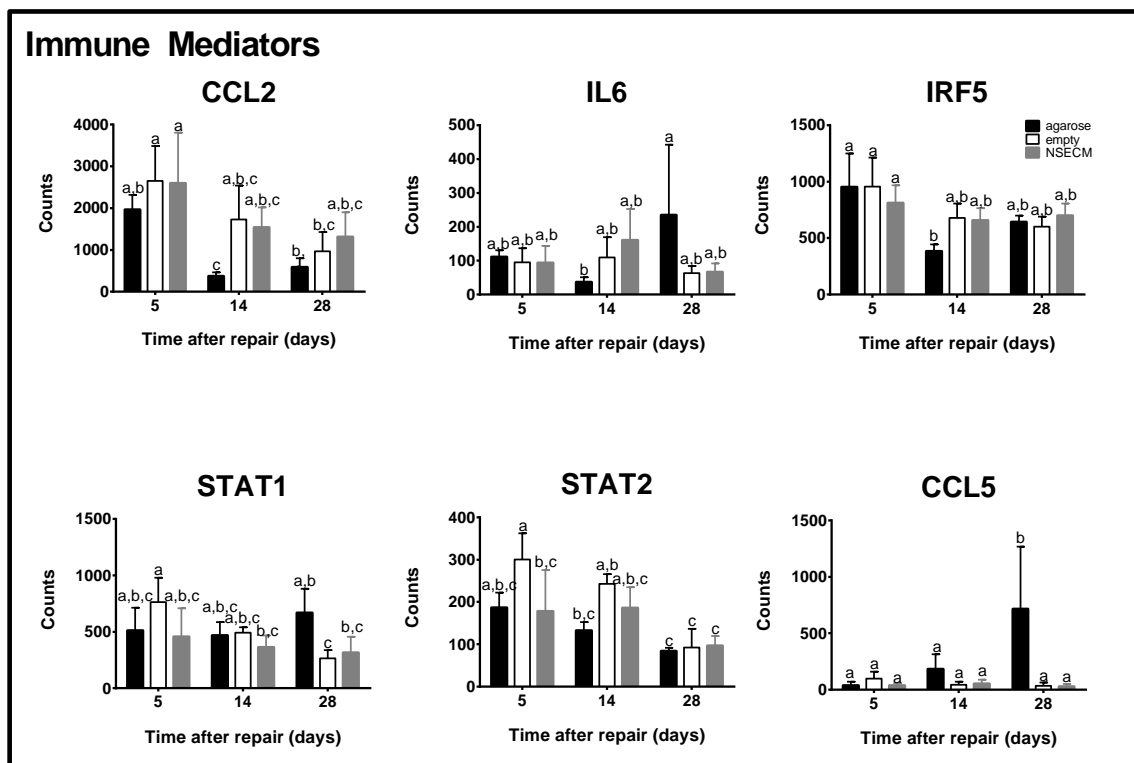


Figure 15: Immune mediators and negative regulators. Groups not connected by the same letter are significantly different ($p < 0.05$, Tukey's post hoc test).

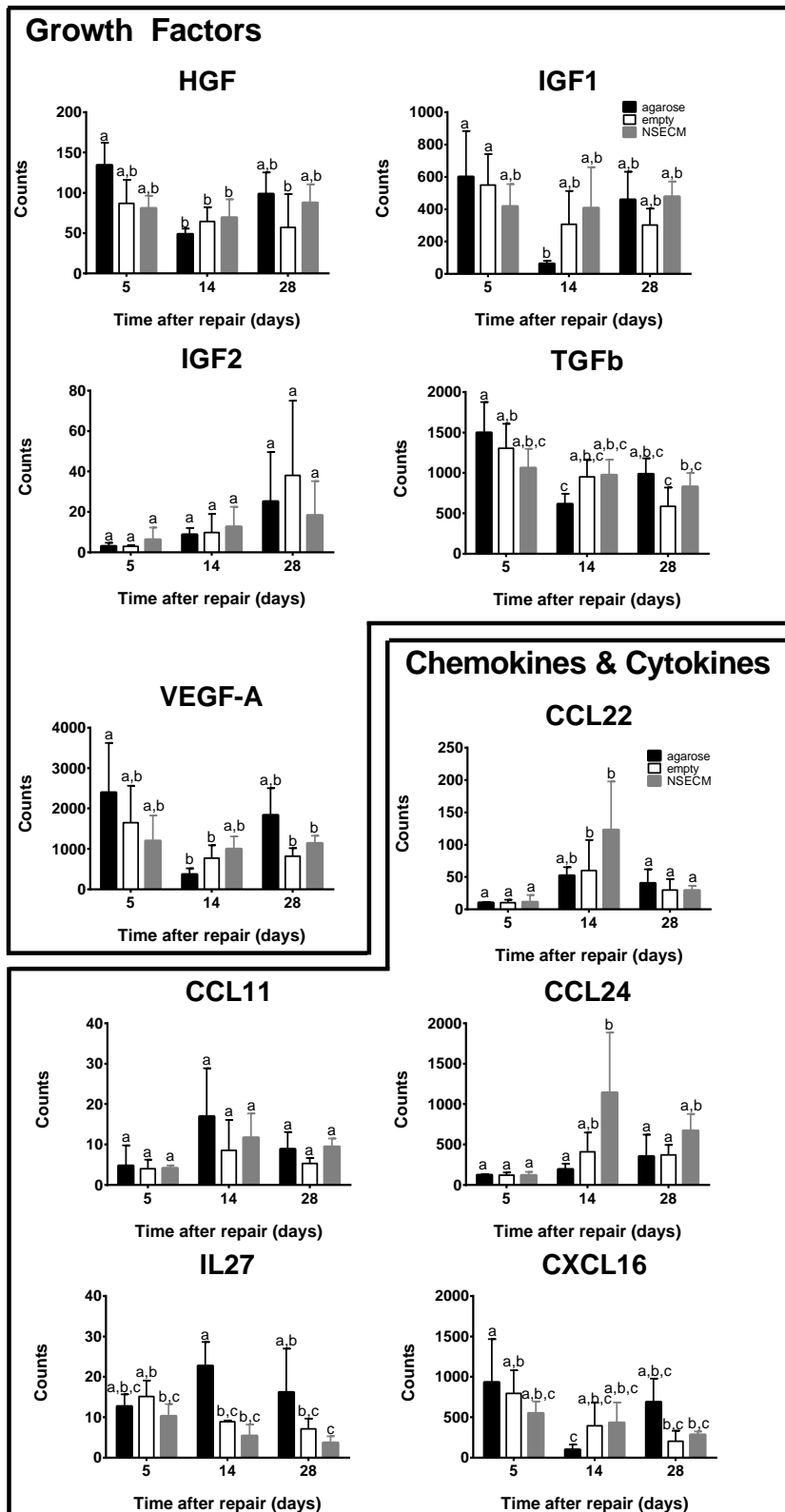


Figure 16: Growth factor, cytokine, and chemokine expression. Groups not connected by the same letter are significantly different ($p < 0.05$, Tukey's post hoc test).

Retrograde Labeling of Regenerated Motor Neurons

To evaluate the functional effects of immune modulation on peripheral nerve regeneration, motor neuron regeneration was quantified at 2, 4, and 8 weeks after injury and repair. This outcome measure evaluated the functional regenerative response to the experimental groups using a retrograde fluorescent tracer to label the cell bodies of motor neurons with axons bridging the gap defect within the conduit. This assessment is functionally important as measurement of axon numbers on cross-section may suggest increased regeneration if profound axonal sprouting is present. For example, studies assessing exogenous glial cell and brain-derived neurotropic factors (GDNF and BDNF) demonstrated sprouting after immediate nerve repair but not an increase the number of motor neurons that regenerate their axons and reach the target muscle (Boyd, 2003; Streppel et al., 2002). This is important as the number of motor neurons (MN) regenerating their axons corresponds to motor unit number and so functional recovery (Wood et al., 2011). Figure 17 shows that by 2 weeks after repair, there was no difference in average regeneration in mice with empty conduit repairs (average 125.6 motor neurons, S.D. 47.3), agarose-filled conduits (average 1.4, S.D. 3.1) or NSECM- filled conduits (average 38.3, S.D. 68.8). By 4 weeks after repair, there was a significant increase in motor neuron numbers in all groups compared to groups at 2 weeks (agarose 502.6 average, S.D. 220.4; empty 505 average, S.D. 155.4; NSECM 552.6 average, S.D. 62.3; $p < 0.05$, Tukey's HSD). There was no difference in motor neuron regeneration between experimental groups at 4 weeks. At 8 weeks after regeneration, there was no further improvement in regeneration compared to 4 weeks. There were also no significant differences in motor neuron count between experimental groups at 8 weeks (agarose 657.7 average, S.D. 96.5; empty 680 average, S.D. 236.4; NSECM 602 average, S.D. 78.6).

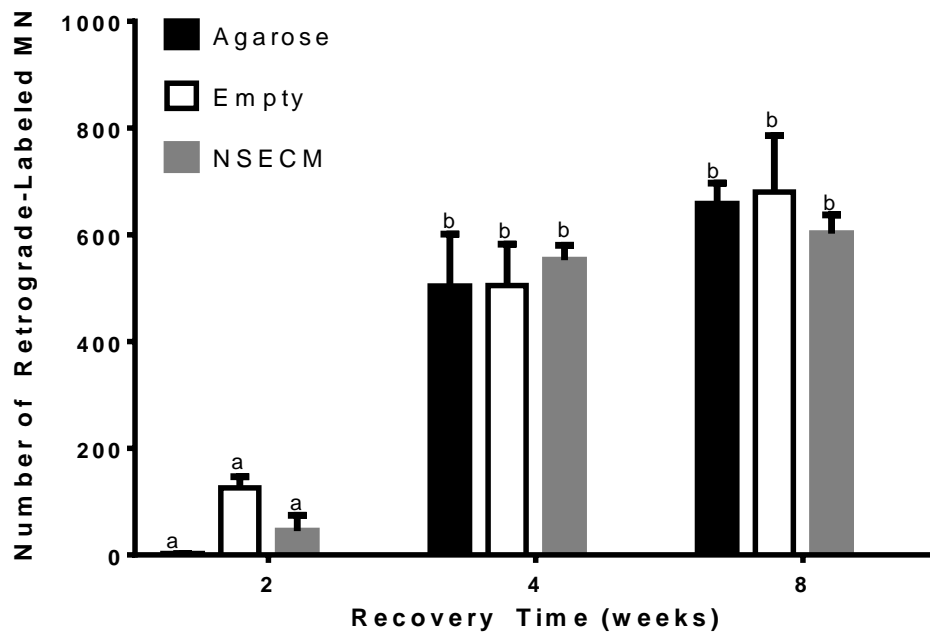


Figure 17: Retrograde-labeled motor neuron counts after 2-8 weeks of recovery. Groups that are not connected by the same letter are significantly different.

DISCUSSION

Peripheral nerve regeneration is dependent both on early inflammatory and neurodegenerative events following injury as well as negative regulators and pro-regenerative processes providing a trophic environment, but the balance between these processes is unclear. Our goals were to define the effects of a novel ECM hydrogel on macrophage function and to evaluate macrophage gene expression after nerve injury in the presence and absence of this hydrogel.

Macrophage gene expression analysis revealed that NSECM promotes a phenotype that is distinct from M2. Where the control M1 (LPS and IFN γ stimulated) and M2 (IL-4 stimulated) controls, representing extremes of in vitro macrophage polarization, largely correspond to previously reported literature, NSECM-stimulated macrophages shared characteristics of both the M1 and M2 expression profile and assumed unique characteristics seen in neither control. Of particular interest is the significant increase in platelet-derived growth factor β (PDGF β) expression in NSECM-stimulated cells. PDGF β protein is a growth factor that contributes to healing and angiogenesis (Pinsky et al., 1995; Risau, 1997; Sato et al., 1993; Spiller et al., 2014). Recent research has reported that early macrophage-driven angiogenesis is a critical factor in regeneration of injured peripheral nerves, as the establishment of a microcapillary network encourages Schwann cell migration to the regenerative bridge (Cattin et al., 2015). The expression patterns seen in the control M1 and M2 cultures further substantiate previously cited findings, with the exception of a few genes. These observations too may be substantiated as these gene expression patterns follow complex signaling pathways that drive expression beyond the signaling of exogenously-applied immune ligands. For example, IL4 receptor α is widely cited as an M2-related gene product, yet expression of the *IL4ra* gene in this study is significantly higher in M1 macrophages but no different in M2 macrophages relative to M0. This phenomenon may reflect the action of a negative-feedback mechanism downregulating the expression of *IL4ra* in M2 as it is stimulated with high mRNA counts of exogenous IL4;

increased expression in M1 may reflect endogenous negative regulator pathways in a highly inflammatory LPS and IFN γ -driven environment. Likely these variations in gene expression profiles in the control samples reflect an overly simplistic M1/M2 dichotomy in a highly variable biological model.

In order to evaluate macrophage gene expression *in vivo*, we developed a method to isolate macrophages from regenerating nerves and applied the same high-throughput transcriptomics assay used *in vitro* to evaluate expression of 90 genes of interest. This novel approach uses multiple cell surface markers to identify macrophages and a range of exclusion markers to allow more specific interrogation of changes in macrophage gene expression after injury than has previously been possible (Day et al., 2014; Fujioka, Purev, Kremlev, Ventura, & Rostami, 2000; Liou, Yuan, Mao, Lai, & Day, 2012). This approach will allow detailed evaluation of the effects of specific manipulations – gene deletion, changing microenvironment mechanics, immunomodulation – in future work.

In contrast to the results seen in the *in vitro* model of macrophage gene expression, macrophages *in vivo* had an unclear distinction between NSECM-treated and control (empty), although there were some clear differences between NSECM and agarose groups. Hierarchical clustering suggests that empty and NSECM experimental groups are more similar than are NSECM and agarose, both which are hydrogels. As we investigated individual gene expression, taking into consideration a few of the selected genes, such as *Arg1*, *iNOS2*, *CD206*, and *TNF*, it would appear that gene expression profiles in the murine model represent an M2-like phenotype early in nerve injury, followed by development of more M1-like genes at later time points in all treatment groups.

These changes in early macrophage gene expression are consistent with recent work suggesting tight immunomodulation through negative regulators of inflammation driving a

predominantly anti-inflammatory environment during the early immune response to injury and prior to cellular infiltration, which may be neuroprotective (Ydens et al., 2012). This is in contrast to earlier work suggesting that the initial response to injury is predominantly pro-inflammatory (de la Hoz, Oliveira, Queiroz, & Langone, 2003; Liefner et al., 2000; Sawada et al., 2007).

Overall, gene expression decreased beyond day 5, which may signify a dampening of the inflammatory signals past the acute phase of Wallerian degeneration and cellular infiltration. Interestingly, several genes showed either a transient increase or decrease in expression at day 14. Broadly, those genes that transiently increased at day 14, such as M1-genes *CCR7* and *CXCL9*, chemokine *CCL11*, and receptor *CCR2*, may be considered “pro-inflammatory”, and those that transiently decreased at day 14, such as negative regulator and transcription factor *NFKBIZ*, and growth factors *IGF-1* and *VEGF-A* could be considered “pro-regenerative.” These transient but significant changes in expression coincided with the time when macrophage numbers increased.

Significant variation in time kinetics between experimental groups was also observed. Agarose groups were found to have more pronounced changes in expression over time, in contrast to relatively stable gene expression patterns over time in the NSECM groups. Agarose treated macrophages tended to correspond to greater increases in M1 (*iNos2*, *TNF*, *IL6*) or immune mediator (*CCL5*) expression and larger decreases M2 (*Arg1*, *CD206*, *Chi3l3*) or negative regulator of inflammation expression (*STAT6*) which also forms part of the IL-4R pathway (M2 associated). These more pronounced changes suggest that agarose may amplify the murine response to injury. There is increasing evidence in support of macrophage phenotypic regulation by physical and mechanical cues (Refai, Textor, Brunette, & Waterfield, 2004; McWhorter, Davis, & Liu, 2014; Van Goethem et al., 2011). Although agarose promotes motor neuron extension *in vitro* (Balgude, Yu, Szymanski, & Bellamkonda, 2001), very little work has

been done to evaluate the effects of substrate stiffness *in vivo*. This forms the basis for ongoing work.

Although NSECM promoted a distinct phenotype *in vitro*, modest effects on gene expression were identified *in vivo*. NSECM was associated with a decrease in M1 (CD68+ CCR7+) macrophage accumulation based on IHC 5 days after injury although no change in M2 (CD68+ CD206+) was observed. Additional analyses on macrophage accumulation in the mid and distal regenerative bridges are ongoing, as well as analyses of macrophage accumulation in agarose-filled conduits.

Macrophages in the regenerating nerve are known to have a profound effect on Schwann cells. In order to complete analysis characterizing the effects of macrophages in the injured peripheral nerve, ongoing work is also evaluating changes in Schwann cell migration and gene expression over time in the same experimental groups.

Motor neuron regeneration showed no differences between treatment and control groups in functional regenerative capacity. Without this distinction, it is difficult to ascribe a functional effect to the macrophage gene expression patterns seen *in vivo*. However, we did see a clear progression of regeneration from 2 to 8 weeks after repair.

Sample size was a limitation in this study. Many of the gene expression analyses show visual differences that were not statistically significant, suggesting that the analysis may be underpowered. Immunohistochemical analyses also showed large standard deviations with small sample sizes; ongoing analyses may strengthen these results.

Previous experiments performed in rats in acute sciatic repair showed increased recovery using NSECM by measuring axon extension and SC migration. (Prest *et al* 2015, in review). We did not observe increases in functional recovery using NSECM in a murine model by measuring motor neuron regeneration. Further, our immunohistochemical analyses are not in line with

previous reports that ECM scaffolds increase M2-like macrophage migration into the scaffold (Prest et al., 2015, in review) (Badylak, Valentin, Ravindra, McCabe, & Stewart-Akers, 2008; Brown et al., 2012, 2009; Ren et al., 2015). We have found that NSECM is associated with a decrease in M1 like macrophages 5 days after injury, although there were no changes in M2 macrophage accumulation. Differences between this and previous studies may be due to the murine environment in peripheral nerve injury showing an inherent M2 bias, thus limiting any further functional effect in macrophage phenotype from NSECM.

Although macrophages are often categorized as M1 or M2, such strict classification can be problematic. Macrophage activation exists on a spectrum, and although distinct differences are observed through stimulation of *in vitro* macrophages with selected immune-related ligands, *in vivo* activation states do not reflect the overly-simplistic M1 (classically activated, pro-inflammatory) and M2 (alternatively activated, regenerative) phenotypes described *in vitro* (Martinez & Gordon, 2014). Macrophages *in vivo* exist in mixed populations and can be individually pleiotropic, with anti-inflammatory signals titrating pro-inflammatory signals to yield a complex inflammatory profile that defies the categorical labels. Ascribing the M1/M2 dichotomy to *in vivo* paradigms fits a simplistic categorical schema to a complex system with the assumption that some proportion of the population will adhere to the scheme, represent a population bias, and generally describe a broad function (Martinez & Gordon, 2014).

Previous work investigating macrophage function in peripheral nerve repair has relied on immunohistochemical analyses or other low-throughput analyses such as qRT-PCR, ELISA, or flow cytometry to identify subsets of a population using a few characteristic markers (Badylak et al., 2008; Brown et al., 2012, 2009; Mokarram et al., 2012; Shechter et al., 2009; Spiller et al., 2014; Taskinen et al., 2000). While these methods have advantages, they are reliant on a pre-genomic era definition of macrophage phenotype based on a few markers, and may be too simplistic to accurately portray the complexity of heterogeneous macrophage populations during

the inflammatory processes accompanying tissue injury and repair. With the understanding that macrophage activation exists on a spectrum with complex inflammatory profiles, it is imperative that outcome measures can appropriately evaluate the heterogeneity of a population of cells. In order to characterize these complex profiles, transcriptomics, proteomics, and secretomics can be employed to evaluate and draw conclusions about macrophage function and regeneration.

In summary, we have shown that NSECM promotes a distinct phenotype *in vitro* but has modest effects *in vivo*. We have shown that gene expression profiles in the murine model represent an M2-like phenotype early in nerve injury, followed by development of more M1-like gene expression profiles at later time points. These changes are more pronounced in macrophages treated with agarose, while mRNA counts tend to be more stable in NSECM-treated macrophages. We have also shown that NSECM decreases the accumulation of M1 macrophages in the regenerative bridge, measured by immunohistochemistry, but the accumulation of M2 macrophages is not affected by NSECM, compared to the control. We have also shown that experimental groups did not affect functional regeneration in the mouse. Lastly, we improved analysis of heterogeneous macrophage populations by isolating macrophages using FACS and using NanoString high-throughput gene expression analysis to interrogate changes in macrophage gene expression after peripheral nerve injury.

APPENDIX

M2 Gene Expression Profile

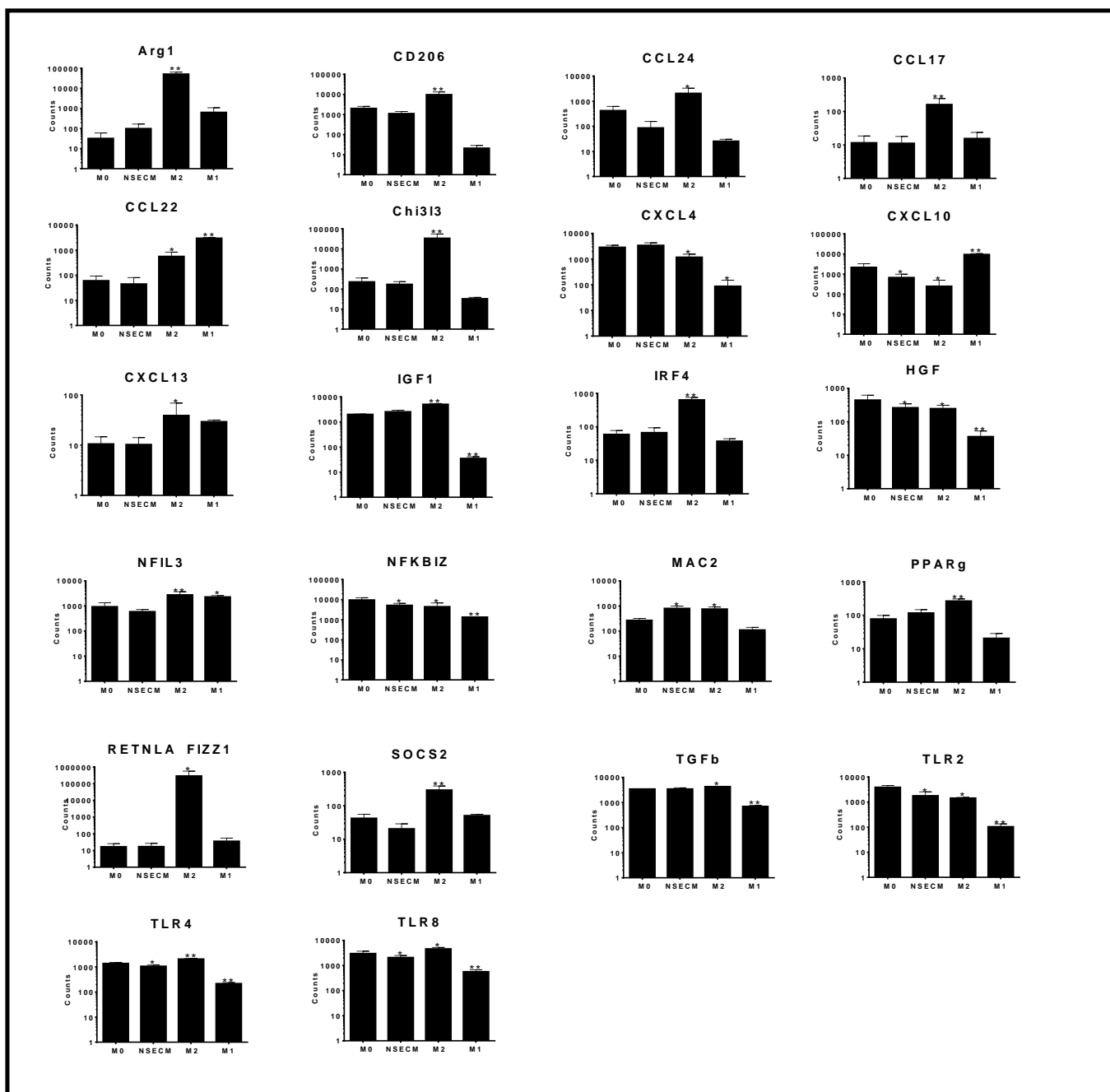


Figure 18. M2 (IL-4) stimulated gene expression analysis of cultured macrophages. *p<0.05, **p<0.0001

M1 Gene Expression Profile

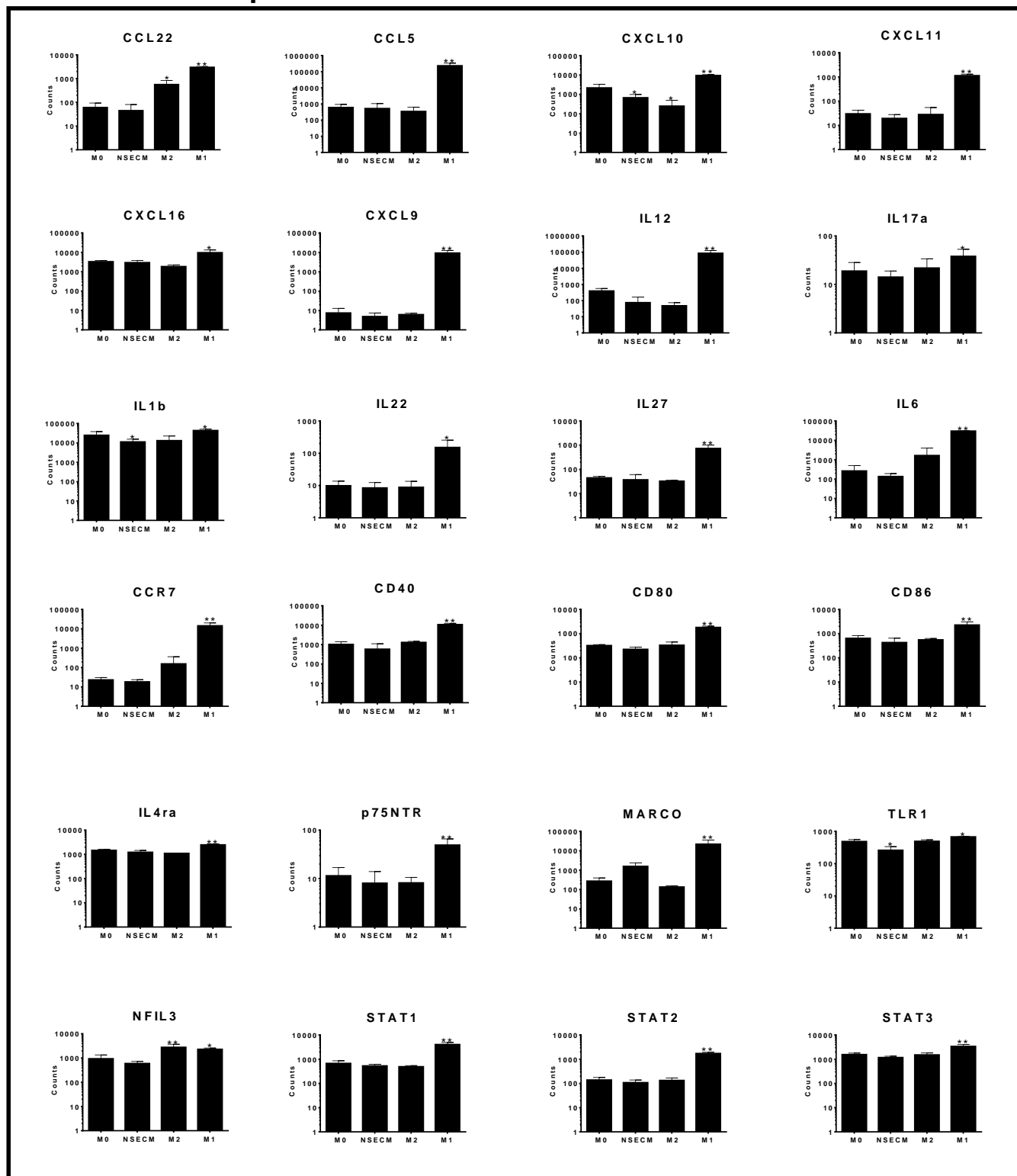


Figure 19. M1 (LPS & IFN γ) stimulated gene expression analysis of cultured macrophages.

*p<0.05, **p<0.0001

M1 Gene Expression Profile

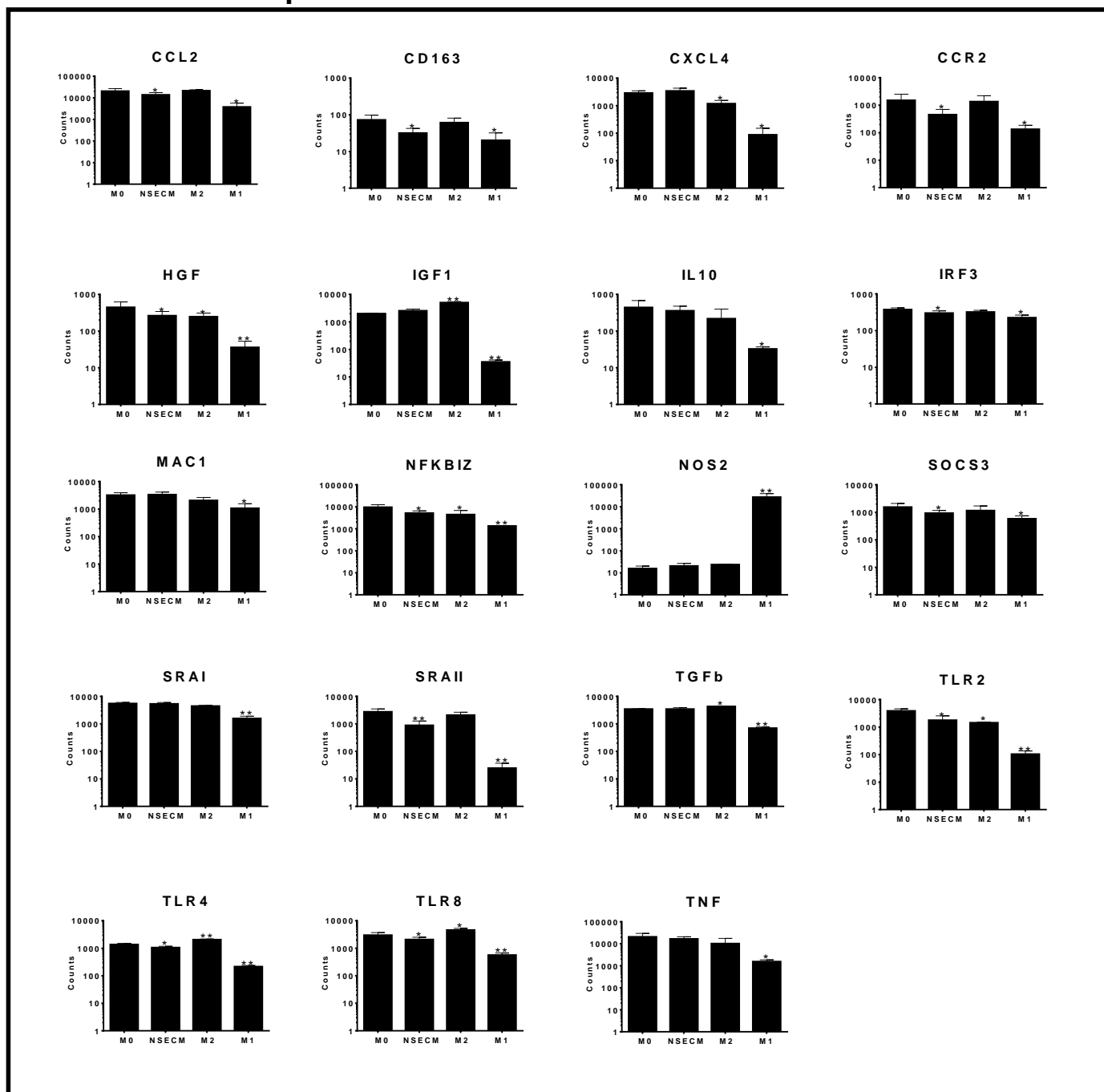


Figure 20. M1 (LPS & IFN γ) stimulated gene expression analysis of cultured macrophages.
*p<0.05, **p<0.0001

Table 6: Sorted macrophage average gene expression data & FDR p-values. Nd denotes no data; samples excluded as mRNA counts were below background expression.

Gene Name	Agarose			Empty			NSECM			FDR p-values		
	5	14	28	5	14	28	5	14	28	Group*Time	Group	Time
Chemokine												
Ccl11	4.70	16.93	8.87	4.04	8.58	5.33	4.13	11.65	9.42	7.53E-01	3.21E-01	2.45E-02
Ccl17	3.64	18.07	16.62	2.89	19.15	22.59	21.09	32.36	9.55	6.67E-01	7.04E-01	4.05E-01
Ccl2	1962.10	368.57	584.31	2647.62	1726.47	965.61	2592.18	1539.24	1313.58	7.36E-01	1.82E-02	1.60E-04
Ccl22	10.07	52.01	40.26	10.50	60.12	30.02	11.01	122.78	29.05	1.51E-01	3.00E-01	4.49E-04
Ccl24	121.10	191.65	351.29	121.55	408.93	370.96	117.23	1139.65	669.39	8.31E-02	1.31E-02	8.71E-03
Ccl5	37.90	183.59	714.97	99.39	44.24	35.59	37.38	53.04	28.48	1.35E-02	1.20E-02	8.33E-02
Cxcl10	153.26	301.51	187.44	252.63	282.51	151.73	169.60	174.54	96.55	5.29E-01	1.38E-01	5.73E-02
CXCL11	4.74	13.96	8.86	7.58	11.06	4.58	4.52	7.51	3.65	nd	nd	nd
CXCL13	7.56	1.88	5.90	6.05	4.92	4.03	7.85	4.44	7.15	nd	nd	nd
Cxcl16	930.79	97.40	687.22	795.17	396.96	202.42	548.87	432.24	284.84	5.56E-02	5.04E-01	4.12E-03
Cxcl4	5621.39	1037.02	724.00	5735.41	1213.12	1582.72	6271.79	1371.25	1400.69	9.95E-01	8.64E-01	1.58E-04
Cxcl9	8.02	117.21	42.41	6.69	2.94	8.12	9.58	4.91	10.06	6.08E-05	5.67E-06	3.45E-03
Cytokine												
CCL1	1.50	2.34	2.96	2.80	1.00	7.57	3.09	2.94	2.93	nd	nd	nd
CCL20	1.18	1.17	2.80	1.35	1.11	4.03	1.45	2.21	2.93	nd	nd	nd
IFNg	4.57	4.25	5.58	3.45	3.19	7.21	2.83	3.16	3.62	nd	nd	nd
Il10	254.74	20.65	116.57	246.54	143.73	106.72	232.10	132.21	131.53	1.48E-01	3.34E-01	1.97E-05
IL12	2.76	2.38	11.37	1.73	3.01	5.09	2.54	5.51	2.93	nd	nd	nd
Il17a	6.90	4.13	7.92	5.74	5.35	8.25	5.13	3.17	6.84	9.94E-01	7.66E-01	2.75E-01
Il1a	719.39	29.90	265.19	471.80	74.47	80.82	258.33	112.54	107.10	4.50E-01	3.46E-01	6.81E-03
Il1b	4417.27	2710.10	4118.76	4675.44	4111.43	3031.71	3632.12	5773.91	2830.05	3.26E-01	9.33E-01	5.55E-01
IL2	2.49	2.44	5.16	3.35	2.44	4.58	2.01	3.40	4.72	nd	nd	nd
IL22	2.12	1.71	4.21	3.33	1.53	4.03	1.87	2.02	3.25	nd	nd	nd

Il23p19	18.72	13.73	28.05	14.18	16.75	12.37	10.36	22.49	13.93	2.21E-01	4.29E-01	6.85E-01
Il27	12.70	22.70	16.14	15.17	8.92	7.15	10.24	5.38	3.65	5.06E-02	3.35E-04	2.18E-01
Il6	110.53	36.34	234.68	95.00	109.14	63.44	93.44	160.49	66.19	4.62E-02	6.64E-01	8.38E-01
Lif	89.60	83.46	101.73	115.56	65.64	52.47	97.69	98.45	40.81	3.72E-01	7.66E-01	2.25E-01
Tnf	1070.85	655.94	1815.27	919.32	1025.30	1203.57	909.90	1077.70	991.55	4.62E-02	5.22E-01	3.21E-02
Enzyme												
Alox15	5.35	2.39	3.94	4.03	2.44	5.16	3.89	2.34	4.77	nd	nd	nd
Arg1	15216.24	320.82	838.14	9725.70	1308.04	604.76	6749.67	3557.42	2639.13	9.81E-04	3.26E-01	4.64E-09
Chi3l3	387.21	19.79	50.80	185.66	117.01	16.93	190.27	370.25	185.82	2.56E-02	9.88E-02	3.92E-02
Nos2	75.10	116.01	364.88	52.72	5.55	15.86	19.29	11.33	8.75	7.78E-02	4.66E-03	2.00E-01
tgm2	1429.16	1890.45	1524.65	1410.24	1216.11	1312.56	1162.20	1315.56	1211.86	6.85E-01	1.05E-01	7.36E-01
Growth Factor												
BDNF	2.92	2.36	9.41	1.97	1.28	4.03	2.79	3.57	2.93	nd	nd	nd
CNTF	13.59	14.54	14.40	12.97	16.86	19.07	12.37	19.59	14.98	4.19E-01	5.32E-01	1.05E-01
EGF	2.44	2.29	2.96	2.68	3.55	4.03	1.53	2.44	5.08	nd	nd	nd
FGF1	5.25	3.42	7.46	5.55	2.75	5.33	2.85	3.73	3.74	nd	nd	nd
FGF2	4.26	4.31	5.60	4.70	3.27	7.82	3.80	4.64	5.08	nd	nd	nd
Gdnf	10.52	14.73	15.88	8.89	18.92	17.20	17.20	11.98	16.69	5.29E-01	8.87E-01	4.56E-01
Hgf	134.12	48.61	98.56	86.97	64.50	57.09	80.83	69.16	87.58	1.05E-01	1.87E-01	1.91E-02
IGF1	599.07	62.18	458.42	549.80	306.34	301.88	416.22	406.54	477.12	9.17E-02	7.66E-01	2.27E-02
IGF2	3.04	8.68	25.14	3.04	9.76	38.01	6.32	12.64	18.21	7.66E-01	8.44E-01	3.60E-02
NGF	3.06	1.94	3.34	1.82	2.17	4.40	2.23	5.14	4.86	nd	nd	nd
NTF3	1.40	1.41	2.80	1.08	2.17	6.88	1.45	1.79	2.93	nd	nd	nd
NTF5	2.20	1.83	3.07	3.37	1.39	5.77	1.48	1.42	3.25	nd	nd	nd
Pdgfb	258.06	230.80	286.65	374.87	328.75	269.99	303.91	279.21	245.58	7.37E-01	3.65E-01	6.17E-01
tgfb	1497.25	614.70	984.52	1305.70	950.91	585.82	1061.79	971.44	826.70	3.06E-02	7.36E-01	3.35E-04
VEGFA	2389.05	366.79	1834.58	1648.67	772.16	820.34	1199.29	995.08	1139.82	1.05E-01	2.75E-01	9.55E-03
Receptor												
Ccr2	571.37	1311.49	571.01	1244.68	2045.68	1061.73	735.38	1941.53	1343.88	3.11E-01	1.46E-03	2.42E-05
CCR7	14.72	34.44	20.63	17.02	62.12	19.07	14.99	110.78	21.38	1.50E-01	1.91E-01	1.33E-03
CD163	36.13	25.61	36.59	83.14	64.94	89.14	390.12	54.67	64.17	6.51E-01	5.09E-01	5.38E-01

CD206	1595.98	188.90	443.66	1384.23	833.95	504.58	1382.30	988.66	874.99	3.71E-01	3.53E-01	1.35E-03
CD40	83.67	66.18	98.22	101.31	108.10	64.41	79.06	98.09	64.40	2.10E-01	7.53E-01	5.44E-01
Cd80	192.21	96.85	151.61	219.14	210.50	104.57	157.17	278.80	158.25	2.71E-02	2.43E-01	1.23E-01
CD86	267.11	363.88	422.75	335.56	439.00	371.96	361.23	454.66	455.82	8.23E-01	3.69E-01	1.05E-01
Il1ra Il1rn	943.75	153.26	1154.23	1000.37	642.97	741.82	792.94	1073.94	995.18	7.78E-02	5.32E-01	1.82E-01
Il4ra	1130.25	121.16	336.07	996.84	418.34	221.40	747.15	581.99	293.09	9.52E-03	9.86E-01	1.35E-07
Mac1	2217.32	94.75	947.37	2190.84	1203.83	549.37	1683.39	1501.74	908.21	1.12E-01	6.85E-01	1.39E-03
Mac2	273.71	310.55	275.62	172.55	168.59	267.69	183.19	185.39	244.82	4.29E-01	1.53E-02	1.97E-01
Marco	37.72	16.09	174.17	51.25	17.95	39.59	58.50	17.21	26.48	5.31E-02	2.15E-01	7.80E-02
NGR	2.29	2.87	4.71	2.15	3.55	5.09	2.29	4.82	4.03	nd	nd	nd
p75NTR	3.71	3.32	3.89	6.25	1.64	4.40	2.97	2.69	5.17	nd	nd	nd
SRAI	1880.83	336.09	800.00	1801.09	822.55	632.03	1472.18	777.94	698.89	2.25E-01	8.32E-01	1.00E-06
SRAII	250.67	87.65	141.83	521.90	283.91	194.73	324.18	210.61	259.08	6.76E-01	1.23E-01	7.85E-02
Tlr1	272.02	102.36	164.96	308.80	210.55	131.31	272.25	203.73	149.32	2.87E-01	4.50E-01	2.48E-04
Tlr2	394.75	252.20	387.05	533.26	334.47	189.97	355.37	301.63	231.79	1.87E-01	6.67E-01	4.78E-02
Tlr4	426.56	16.21	106.19	310.13	139.68	49.72	231.81	167.20	106.39	4.67E-03	8.70E-01	5.33E-07
Tlr8	605.91	271.40	344.55	509.04	377.85	295.84	391.57	383.15	362.06	8.33E-02	8.52E-01	3.24E-03
Secreted Protein												
Retnla	39.16	548.76	555.08	63.35	1309.08	1162.00	31.10	1370.66	1732.25	3.93E-01	5.31E-02	3.35E-04
Signaling Regulator												
Socs1	22.97	8.53	46.49	28.04	21.97	22.95	28.80	24.32	22.85	9.34E-03	9.33E-01	4.64E-02
Socs2	11.14	7.35	17.59	14.06	16.90	11.44	13.05	23.39	27.79	2.02E-01	5.31E-02	2.76E-01
Socs3	741.92	233.71	268.80	636.45	341.79	227.20	645.02	394.60	256.39	4.50E-01	8.82E-01	5.33E-07
Transcription Factor												
Irf3	118.83	52.16	68.27	116.00	71.45	60.25	103.18	69.62	59.21	7.53E-01	9.02E-01	3.35E-04
Irf4	20.90	29.04	50.10	26.24	86.06	79.24	27.17	81.98	107.59	2.33E-01	7.72E-03	2.68E-04
Irf5	951.02	382.75	642.41	955.31	678.95	600.64	811.21	655.68	699.45	1.55E-01	5.32E-01	5.81E-04
Nfil3	1413.08	603.87	1085.18	1085.77	703.53	617.77	906.72	825.67	640.75	1.05E-01	1.05E-01	4.72E-03
Nfkbiz	1548.42	528.11	1202.57	1512.85	1024.40	940.69	1186.84	1114.93	917.84	2.19E-01	8.90E-01	3.46E-02

PPARg	75.65	64.71	68.64	68.64	96.13	70.57	67.72	89.98	99.93	4.44E-01	4.29E-01	5.75E-01
Sbno2	588.26	244.71	319.78	485.73	341.87	301.35	482.16	406.48	307.24	1.02E-01	8.58E-01	2.56E-05
Stat1	510.83	467.85	667.31	763.60	492.21	266.04	455.60	363.06	315.49	3.11E-02	1.08E-01	1.20E-01
Stat2	186.33	132.77	83.66	300.12	242.59	92.35	178.09	185.84	96.41	1.26E-01	8.71E-03	2.07E-05
Stat3	1053.52	187.13	475.50	814.72	462.11	277.71	669.81	543.70	411.43	3.82E-02	8.58E-01	6.25E-05
Stat6	569.54	299.41	349.24	501.96	391.71	280.91	432.62	422.83	286.58	1.50E-01	8.50E-01	3.65E-04

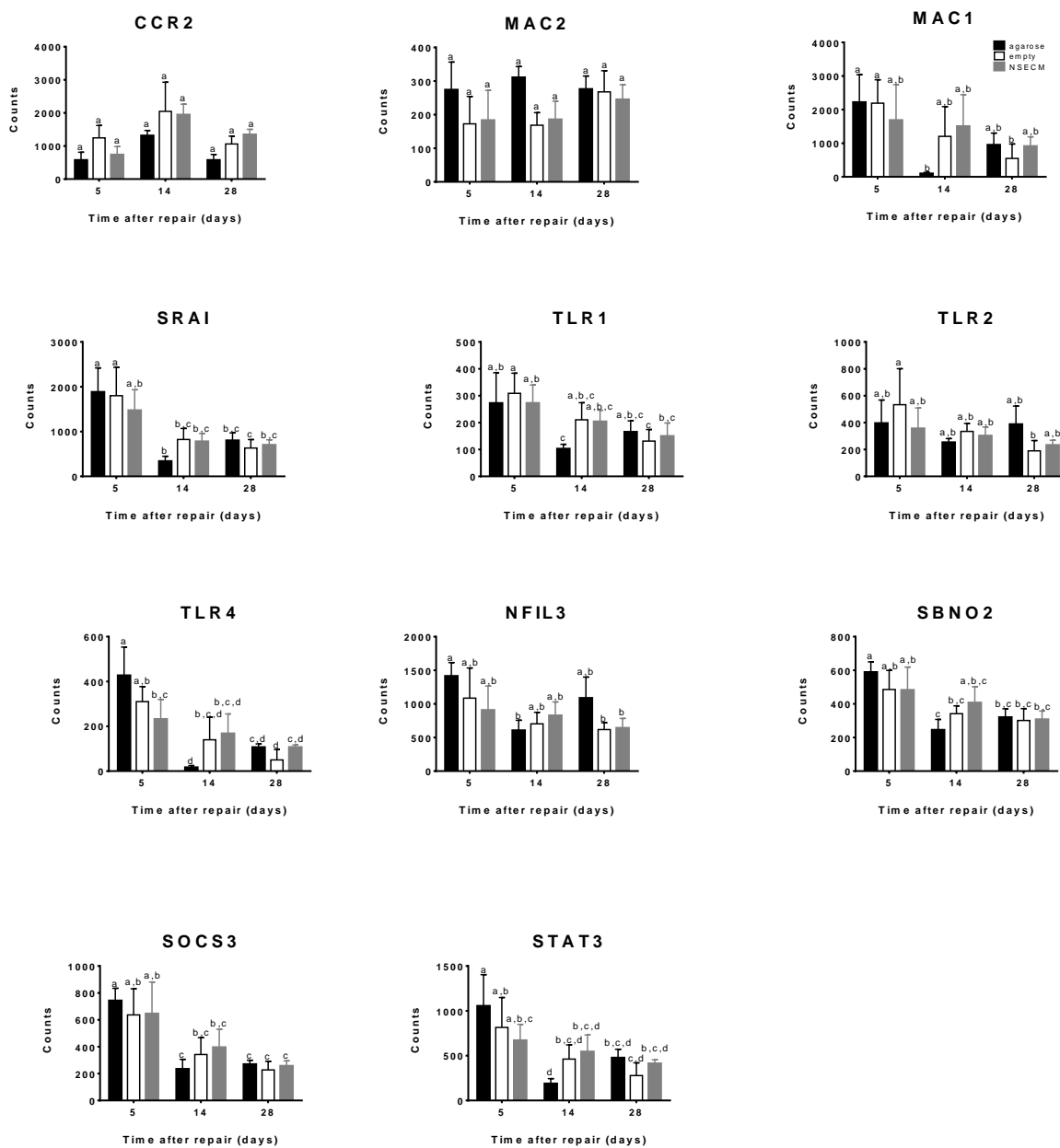


Figure 21: Receptor, transcription factor, and cytokine regulator gene analysis of *in vivo* macrophages. Groups not connected by the same letter are significantly different ($p < 0.05$, Tukey's post hoc test).

REFERENCES

- Al-Majed, a a, Neumann, C. M., Brushart, T. M., & Gordon, T. (2000). Brief electrical stimulation promotes the speed and accuracy of motor axonal regeneration. *The Journal of Neuroscience : The Official Journal of the Society for Neuroscience*, *20*(7), 2602–2608.
- Badylak, S. F. (2004). Xenogeneic extracellular matrix as a scaffold for tissue reconstruction. *Transplant Immunology*, *12*(3-4), 367–377. doi:10.1016/j.trim.2003.12.016
- Badylak, S. F., Valentin, J. E., Ravindra, A. K., McCabe, G. P., & Stewart-Akers, A. M. (2008). Macrophage phenotype as a determinant of biologic scaffold remodeling. *Tissue Engineering. Part A*, *14*(11), 1835–42. doi:10.1089/ten.tea.2007.0264
- Baichwal, R. R., Bigbee, J. W., & DeVries, G. H. (1988). Macrophage-mediated myelin-related mitogenic factor for cultured Schwann cells. *Proceedings of the National Academy of Sciences of the United States of America*, *85*(5), 1701–5. Retrieved from <http://www.pubmedcentral.nih.gov/articlerender.fcgi?artid=279842&tool=pmcentrez&render type=abstract>
- Bailey, S. B., Eichler, M. E., Villadiego, a, & Rich, K. M. (1993). The influence of fibronectin and laminin during Schwann cell migration and peripheral nerve regeneration through silicon chambers. *Journal of Neurocytology*, *22*(3), 176–84. doi:10.1007/BF01246356
- Balgude, A. P., Yu, X., Szymanski, A., & Bellamkonda, R. V. (2001). Agarose gel stiffness determines rate of DRG neurite extension in 3D cultures. *Biomaterials*, *22*(10), 1077–1084. doi:10.1016/S0142-9612(00)00350-1
- Barrette, B., Hébert, M.-A., Filali, M., Lafortune, K., Vallières, N., Gowing, G., ... Lacroix, S. (2008). Requirement of myeloid cells for axon regeneration. *The Journal of Neuroscience : The Official Journal of the Society for Neuroscience*, *28*(38), 9363–9376. doi:10.1523/JNEUROSCI.1447-08.2008
- Bell, J. H. a., & Haycock, J. W. (2012). Next Generation Nerve Guides: Materials, Fabrication, Growth Factors, and Cell Delivery. *Tissue Engineering Part B: Reviews*, *18*(2), 116–128. doi:10.1089/ten.teb.2011.0498
- Beuche, W., & Friede, R. L. (1984). The role of non-resident cells in Wallerian degeneration. *Journal of Neurocytology*, *13*(5), 767–796. doi:10.1007/BF01148493
- Boyd, J. (2003). Glial cell line-derived neurotrophic factor and brain-derived neurotrophic factor sustain the axonal regeneration of chronically axotomized motoneurons in vivo. *Experimental Neurology*, *183*(2), 610–619. doi:10.1016/S0014-4886(03)00183-3
- Brown, B. N., Chung, W. L., Pavlick, M., Reppas, S., Ochs, M. W., Russell, A. J., & Badylak, S. F. (2011). Extracellular matrix as an inductive template for temporomandibular joint meniscus reconstruction: a pilot study. *Journal of Oral and Maxillofacial Surgery : Official Journal of the American Association of Oral and Maxillofacial Surgeons*, *69*(12), e488–505. doi:10.1016/j.joms.2011.02.130

- Brown, B. N., Londono, R., Tottey, S., Zhang, L., Kukla, K. A., Wolf, M. T., ... Badylak, S. F. (2012). Acta Biomaterialia Macrophage phenotype as a predictor of constructive remodeling following the implantation of biologically derived surgical mesh materials. *Acta Biomaterialia*, 8(3), 978–987. doi:10.1016/j.actbio.2011.11.031
- Brown, B. N., Valentin, J. E., Stewart-akers, A. M., McCabe, G. P., & Badylak, S. F. (2009). Biomaterials Macrophage phenotype and remodeling outcomes in response to biologic scaffolds with and without a cellular component. *Biomaterials*, 30(8), 1482–1491. doi:10.1016/j.biomaterials.2008.11.040
- Cattin, A.-L., Burden, J. J., Van Emmenis, L., Mackenzie, F. E., Hoving, J. J. A., Garcia Calavia, N., ... Lloyd, A. C. (2015). Macrophage-Induced Blood Vessels Guide Schwann Cell-Mediated Regeneration of Peripheral Nerves. *Cell*, 162(5), 1127–1139. doi:10.1016/j.cell.2015.07.021
- Chen, P., Piao, X., & Bonaldo, P. (2015). Role of macrophages in Wallerian degeneration and axonal regeneration after peripheral nerve injury. *Acta Neuropathologica*. doi:10.1007/s00401-015-1482-4
- Chen, Y. Y., McDonald, D., Cheng, C., Magnowski, B., Durand, J., & Zochodne, D. W. (2005). Axon and Schwann cell partnership during nerve regrowth. *Journal of Neuropathology and Experimental Neurology*, 64, 613–622. doi:10.1097/01.jnen.0000171650.94341.46
- Corfas, G., Velardez, M. O., Ko, C.-P., Ratner, N., & Peles, E. (2004). Mechanisms and roles of axon-Schwann cell interactions. *The Journal of Neuroscience : The Official Journal of the Society for Neuroscience*, 24(42), 9250–9260. doi:10.1523/JNEUROSCI.3649-04.2004
- Cornbrooks, C. J., Carey, D. J., McDonald, J. a, Timpl, R., & Bunge, R. P. (1983). In vivo and in vitro observations on laminin production by Schwann cells. *Proceedings of the National Academy of Sciences of the United States of America*, 80(12), 3850–4. doi:10.1073/pnas.80.12.3850
- Day, Y.-J., Liou, J.-T., Lee, C.-M., Lin, Y.-C., Mao, C.-C., Chou, A.-H., ... Lee, H.-C. (2014). Lack of interleukin-17 leads to a modulated micro-environment and amelioration of mechanical hypersensitivity after peripheral nerve injury in mice. *Pain*, 155(7), 1293–302. doi:10.1016/j.pain.2014.04.004
- de la Hoz, C. L. R., Oliveira, A. L. R., Queiroz, L. D. S., & Langone, F. (2003). Wallerian degeneration in C57BL/6J and A/J mice: differences in time course of neurofilament and myelin breakdown, macrophage recruitment and iNOS expression. *Journal of Anatomy*, 203(6), 567–78. Retrieved from <http://www.pubmedcentral.nih.gov/articlerender.fcgi?artid=1571200&tool=pmcentrez&rendertype=abstract>
- Deumens, R., Bozkurt, A., Meek, M. F., Marcus, M. a. E., Joosten, E. a. J., Weis, J., & Brook, G. a. (2010). Repairing injured peripheral nerves: Bridging the gap. *Progress in Neurobiology*, 92(3), 245–276. doi:10.1016/j.pneurobio.2010.10.002

- Elkabes, S., DiCicco-Bloom, E. M., & Black, I. B. (1996). Brain microglia/macrophages express neurotrophins that selectively regulate microglial proliferation and function. *The Journal of Neuroscience : The Official Journal of the Society for Neuroscience*, *16*(8), 2508–2521.
- Frostick, S. P., Yin, Q., & Kemp, G. J. (1998). Schwann cells, neurotrophic factors, and peripheral nerve regeneration. *Microsurgery*, *18*, 397–405. doi:10.1002/(SICI)1098-2752(1998)18:7<397::AID-MICR2>3.0.CO;2-F [pii]
- Fu, S. Y., & Gordon, T. (1995). Contributing factors to poor functional recovery after delayed nerve repair: prolonged denervation. *The Journal of Neuroscience : The Official Journal of the Society for Neuroscience*, *15*(5 Pt 2), 3886–3895.
- Fu, S. Y., & Gordon, T. (1997). The cellular and molecular basis of peripheral nerve regeneration. *Molecular Neurobiology*, *14*(1), 67–116. doi:10.1007/BF02740621
- Fujioka, T., Purev, E., Kremlev, S. G., Ventura, E. S., & Rostami, A. (2000). Flow cytometric analysis of infiltrating cells in the peripheral nerves in experimental allergic neuritis. *Journal of Neuroimmunology*, *108*, 181–191. doi:10.1016/S0165-5728(00)00270-8
- Gaudet, A. D., Popovich, P. G., & Ramer, M. S. (2011). Wallerian degeneration: gaining perspective on inflammatory events after peripheral nerve injury. *Journal of Neuroinflammation*, *8*(1), 110. doi:10.1186/1742-2094-8-110
- Ghalib, N., Houst'ava, L., Haninec, P., & Dubovy, P. (2001). Morphometric analysis of early regeneration of motor axons through motor and cutaneous nerve grafts. *Annals of Anatomy = Anatomischer Anzeiger : Official Organ of the Anatomische Gesellschaft*, *183*(4), 363–368. doi:10.1016/S0940-9602(01)80183-7
- Gordon, T., Tyreman, N., & Raji, M. a. (2011). The basis for diminished functional recovery after delayed peripheral nerve repair. *The Journal of Neuroscience : The Official Journal of the Society for Neuroscience*, *31*(14), 5325–5334. doi:10.1523/JNEUROSCI.6156-10.2011
- Griffin, J. W., Hogan, M. V, Chhabra, a B., & Deal, D. N. (2013). Peripheral nerve repair and reconstruction. *The Journal of Bone and Joint Surgery. American Volume*, *95*(23), 2144–51. doi:10.2106/JBJS.L.00704
- Hall, S. M. (1986a). Regeneration in cellular and acellular autografts in the peripheral nervous system. *Neuropathology and Applied Neurobiology*, *12*(1), 27–46. Retrieved from <http://www.ncbi.nlm.nih.gov/pubmed/3703154>
- Hall, S. M. (1986b). The effect of inhibiting Schwann cell mitosis on the re-innervation of acellular autografts in the peripheral nervous system of the mouse. *Neuropathology and Applied Neurobiology*, *12*(4), 401–414.
- Hall, S. M. (1989). Regeneration in the peripheral nervous system. *Neuropathol Appl Neurobiol*, *15*(6), 513–529. Retrieved from http://www.ncbi.nlm.nih.gov/entrez/query.fcgi?cmd=Retrieve&db=PubMed&dopt=Citation&list_uids=2693992

- Heumann, R., Lindholm, D., Bandtlow, C., Meyer, M., Radeke, M. J., Misko, T. P., ... Thoenen, H. (1987). Differential regulation of mRNA encoding nerve growth factor and its receptor in rat sciatic nerve during development, degeneration, and regeneration: role of macrophages. *Proc Natl Acad Sci Usa*, *84*(8735), 8735–8739.
- Jessen, K., & Mirsky, R. (2005). The origin and development of glial cells in peripheral nerves, 6(September). doi:10.1038/nrn1746
- Khuong, H. T., Kumar, R., Senjaya, F., Grochmal, J., Ivanovic, A., Shakhbazau, A., ... Midha, R. (2014). Skin derived precursor Schwann cells improve behavioral recovery for acute and delayed nerve repair. *Experimental Neurology*, *254*, 168–179. doi:10.1016/j.expneurol.2014.01.002
- Kouyoumdjian, J. A. (2006). Peripheral nerve injuries: A retrospective survey of 456 cases. *Muscle and Nerve*, *34*(6), 785–788. doi:10.1002/mus.20624
- Lavasani, M., Thompson, S. D., Pollett, J. B., Usas, A., Lu, A., Stolz, D. B., ... Huard, J. (2014). Human muscle – derived stem / progenitor cells promote functional murine peripheral nerve regeneration, *124*(4). doi:10.1172/JCI44071.eration
- Li, R., Liu, Z., Pan, Y., Chen, L., Zhang, Z., & Lu, L. (2014). Peripheral Nerve Injuries Treatment: A Systematic Review. *Cell Biochemistry and Biophysics*. doi:10.1007/s12013-013-9742-1
- Liefner, M., Siebert, H., Sachse, T., Michel, U., Kollias, G., & Brück, W. (2000). The role of TNF- α during Wallerian degeneration. *Journal of Neuroimmunology*, *108*(1-2), 147–52. doi:S0165572800002629 [pii]
- Lindholm, D., Heumann, R., Meyer, M., & Thoenen, H. (1987). Interleukin-1 regulates synthesis of nerve growth factor in non-neuronal cells of rat sciatic nerve. *Nature*, *330*(6149), 658–9. doi:10.1038/330658a0
- Liou, J.-T., Yuan, H.-B., Mao, C.-C., Lai, Y.-S., & Day, Y.-J. (2012). Absence of C-C motif chemokine ligand 5 in mice leads to decreased local macrophage recruitment and behavioral hypersensitivity in a murine neuropathic pain model. *Pain*, *153*(6), 1283–91. doi:10.1016/j.pain.2012.03.008
- Lundborg, G., Dahlin, L. B., Danielsen, N., Gelberman, R. H., Longo, F. M., Powell, H. C., & Varon, S. (1982). Nerve regeneration in silicone chambers: influence of gap length and of distal stump components. *Experimental Neurology*, *76*(2), 361–375. doi:10.1016/0014-4886(82)90215-1
- Mackinnon, S. E., Doolabh, V. B., Novak, C. B., & Trulock, E. P. (2001). Clinical outcome following nerve allograft transplantation. *Plastic and Reconstructive Surgery*, *107*(6), 1419–1429.
- Martinez, F. O., & Gordon, S. (2014). The M1 and M2 paradigm of macrophage activation: time for reassessment. *F1000prime Reports*, *6*(March), 13. doi:10.12703/P6-13
- McGrath, J. C., Drummond, G. B., McLachlan, E. M., Kilkenny, C., & Wainwright, C. L. (2010).

- Editorial: Guidelines for reporting experiments involving animals: The ARRIVE guidelines. *British Journal of Pharmacology*, 160(7), 1573–1576. doi:10.1111/j.1476-5381.2010.00873.x
- Midha, R., Munro, C. a, Chan, S., Nitising, A., Xu, Q.-G., & Gordon, T. (2005). Regeneration into protected and chronically denervated peripheral nerve stumps. *Neurosurgery*, 57(6), 1289–1299; discussion 1289–1299. doi:10.1227/01.NEU.0000187480.38170.EC
- Mokarram, N., Merchant, A., Mukhatyar, V., Patel, G., & Bellamkonda, R. V. (2012). Effect of modulating macrophage phenotype on peripheral nerve repair. *Biomaterials*, 33(34), 8793–801. doi:10.1016/j.biomaterials.2012.08.050
- Mueller, M., Leonhard, C., Wacker, K., Ringelstein, E. B., Okabe, M., Hickey, W. F., & Kiefer, R. (2003). Macrophage Response to Peripheral Nerve Injury : The Hematogenous Macrophages, 83(2), 175–185. doi:10.1097/01.LAB.0000056993.28149.BF
- Murray, P. J., Allen, J. E., Biswas, S. K., Fisher, E. a., Gilroy, D. W., Goerdts, S., ... Wynn, T. a. (2014). Macrophage Activation and Polarization: Nomenclature and Experimental Guidelines. *Immunity*, 41(1), 14–20. doi:10.1016/j.immuni.2014.06.008
- Nichols, C. M., Brenner, M. J., Fox, I. K., Tung, T. H., Hunter, D. a, Rickman, S. R., & Mackinnon, S. E. (2004). Effects of motor versus sensory nerve grafts on peripheral nerve regeneration. *Experimental Neurology*, 190(2), 347–55. doi:10.1016/j.expneurol.2004.08.003
- Noble, J., Munro, C. a, Prasad, V. S., & Midha, R. (1998). Analysis of upper and lower extremity peripheral nerve injuries in a population of patients with multiple injuries. *The Journal of Trauma*, 45(1), 116–22. doi:10.1097/00005373-199807000-00025
- Perrin, F. E., Lacroix, S., Avilés-Trigueros, M., & David, S. (2005). Involvement of monocyte chemoattractant protein-1, macrophage inflammatory protein-1alpha and interleukin-1beta in Wallerian degeneration. *Brain : A Journal of Neurology*, 128(Pt 4), 854–866. doi:10.1093/brain/awh407
- Pfister, B. J., Gordon, T., Loverde, J. R., Kochar, A. S., Mackinnon, S. E., & Cullen, D. K. (2011). Biomedical engineering strategies for peripheral nerve repair: surgical applications, state of the art, and future challenges. *Critical Reviews in Biomedical Engineering*, 39(2), 81–124. doi:10.1615/CritRevBiomedEng.v39.i2.20
- Pinsky, D. J., Lyn, P., Leavy, J., Wittet, L., Joseph-silversteint, J., Furie, M. B., ... Stern, D. M. (1995). acidic/basic, 92(May), 4606–4610.
- Portincasa, A., Gozzo, G., Parisi, D., Annacontini, L., Campanale, A., Basso, G., & Maiorella, A. (2007). Microsurgical treatment of injury to peripheral nerves in upper and lower limbs: A critical review of the last 8 years. *Microsurgery*, 27(5), 455–462. doi:10.1002/micr.20382
- Pruszk, J., Ludwig, W., Blak, A., Alavian, K., & Isacson, O. (2012). NIH Public Access, 27(12), 2928–2940. doi:10.1002/stem.211.CD15

- Refai, A. K., Textor, M., Brunette, D. M., & Waterfield, J. D. (2004). Effect of titanium surface topography on macrophage activation and secretion of proinflammatory cytokines and chemokines. *Journal of Biomedical Materials Research. Part A*, *70*, 194–205. doi:10.1002/jbm.a.30075
- Reing, J. E., Zhang, L., Myers-Irvin, J., Cordero, K. E., Freytes, D. O., Heber-Katz, E., ... Badylak, S. F. (2009). Degradation products of extracellular matrix affect cell migration and proliferation. *Tissue Engineering Part A*, *15*(3), 605–614. doi:10.1089/ten.tea.2007.0425
- Ren, T., van der Merwe, Y., & Steketee, M. B. (2015). Developing extracellular matrix technology to treat retinal or optic nerve injury. *eNeuro*. doi:10.1523/ENEURO.0077-15.2015
- Risau, W. (1997). Mechanisms of angiogenesis. *Nature*, *386*(6626), 671–674. doi:10.1146/annurev.physiol.49.1.453
- Sato, N., Beitz, J. G., Kato, J., Yamamoto, M., Clark, J. W., Calabresi, P., ... Frackelton, a R. (1993). Platelet-derived growth factor indirectly stimulates angiogenesis in vitro. *The American Journal of Pathology*, *142*(4), 1119–1130.
- Sawada, T., Sano, M., Omura, T., Omura, K., Hasegawa, T., Funahashi, S., & Nagano, A. (2007). Spatiotemporal quantification of tumor necrosis factor-alpha and interleukin-10 after crush injury in rat sciatic nerve utilizing immunohistochemistry. *Neuroscience Letters*, *417*(1), 55–60. doi:10.1016/j.neulet.2007.02.028
- Scheib, J., & Höke, A. (2013). Advances in peripheral nerve regeneration. *Nature Reviews. Neurology*, *9*(12), 668–76. doi:10.1038/nrneurol.2013.227
- Scholz, T., Krichevsky, A., Sumarto, A., Jaffurs, D., Wirth, G. A., Paydar, K., & Evans, G. R. D. (2009). Peripheral nerve injuries: an international survey of current treatments and future perspectives. *Journal of Reconstructive Microsurgery*, *25*(6), 339–344. doi:10.1055/s-0029-1215529
- Seddon, H. J., Medawar, P. B., & Smith, H. (1943). Rate of regeneration of peripheral nerves in man. *The Journal of Physiology*, *102*(2), 191–215.
- Selecki, B. R., Ring, I. T., Simpson, D. A., Vanderfield, G. K., & Sewell, M. F. (1982). Trauma to the central and peripheral nervous systems: Part I: an overview of mortality, morbidity and costs; N.S.W. 1977. *The Australian and New Zealand Journal of Surgery*, *52*(1), 93–102.
- Shamash, S., Reichert, F., & Rotshenker, S. (2002). The cytokine network of Wallerian degeneration: tumor necrosis factor-alpha, interleukin-1alpha, and interleukin-1beta. *The Journal of Neuroscience : The Official Journal of the Society for Neuroscience*, *22*(8), 3052–3060. doi:20026249
- Shechter, R., London, A., Varol, C., Raposo, C., Cusimano, M., Yovel, G., ... Schwartz, M. (2009). Infiltrating blood-derived macrophages are vital cells playing an anti-inflammatory role in recovery from spinal cord injury in mice. *PLoS Medicine*, *6*(7), e1000113.

doi:10.1371/journal.pmed.1000113

- Spiller, K. L., Anfang, R. R., Spiller, K. J., Ng, J., Nakazawa, K. R., Daulton, J. W., & Vunjak-Novakovic, G. (2014). The role of macrophage phenotype in vascularization of tissue engineering scaffolds. *Biomaterials*, *35*(15), 4477–4488. doi:10.1016/j.biomaterials.2014.02.012
- Sridharan, R., Cameron, A. R., Kelly, D. J., Kearney, C. J., & Brien, F. J. O. (2015). Biomaterial based modulation of macrophage polarization : a review and suggested design principles. *Biochemical Pharmacology*, *18*(6), 313–325. doi:10.1016/j.mattod.2015.01.019
- Streppel, M., Azzolin, N., Dohm, S., Guntinas-Lichius, O., Haas, C., Grothe, C., ... Angelov, D. N. (2002). Focal application of neutralizing antibodies to soluble neurotrophic factors reduces collateral axonal branching after peripheral nerve lesion. *The European Journal of Neuroscience*, *15*(8), 1327–42.
- Subang, M. C., & Richardson, P. M. (2001). Influence of injury and cytokines on synthesis of monocyte chemoattractant protein-1 mRNA in peripheral nervous tissue. *The European Journal of Neuroscience*, *13*(3), 521–8. Retrieved from <http://www.ncbi.nlm.nih.gov/pubmed/11168559>
- Sulaiman, O. A., & Gordon, T. (2000). Effects of short- and long-term Schwann cell denervation on peripheral nerve regeneration, myelination, and size. *Glia*, *32*(3), 234–246. doi:10.1002/1098-1136(200012)32:3<234::AID-GLIA40>3.0.CO;2-3
- Taskinen, H. S., Olsson, T., Buchta, a, Khademi, M., Svelander, L., & Røyttä, M. (2000). Peripheral nerve injury induces endoneurial expression of IFN-gamma, IL-10 and TNF-alpha mRNA. *Journal of Neuroimmunology*, *102*, 17–25. doi:10.1016/S0165-5728(99)00154-X
- Taskinen, H. S., & Røyttä, M. (1997). The dynamics of macrophage recruitment after nerve transection. *Acta Neuropathologica*, *93*(3), 252–9.
- Taylor, C. a, Braza, D., Rice, J. B., & Dillingham, T. (2008). The incidence of peripheral nerve injury in extremity trauma. *American Journal of Physical Medicine & Rehabilitation / Association of Academic Physiatrists*, *87*(5), 381–385. doi:10.1097/PHM.0b013e31815e6370
- Toews, A. D., Barrett, C., & Morell, P. (1998). Monocyte chemoattractant protein 1 is responsible for macrophage recruitment following injury to sciatic nerve. *Journal of Neuroscience Research*, *53*(2), 260–267. doi:10.1002/(SICI)1097-4547(19980715)53:2<260::AID-JNR15>3.0.CO;2-A
- Tofaris, G. K., Patterson, P. H., Jessen, K. R., & Mirsky, R. (2002). Denervated Schwann cells attract macrophages by secretion of leukemia inhibitory factor (LIF) and monocyte chemoattractant protein-1 in a process regulated by interleukin-6 and LIF. *The Journal of Neuroscience : The Official Journal of the Society for Neuroscience*, *22*(15), 6696–6703. doi:20026699

Waller, A. (1850). By M.D. *Philosophical Transactions of the Royal Society of London*, (140), 432–429.

Wood, M. D., Kemp, S. W. P., Weber, C., Borschel, G. H., & Gordon, T. (2011). Outcome measures of peripheral nerve regeneration. *Annals of Anatomy = Anatomischer Anzeiger : Official Organ of the Anatomische Gesellschaft*, 193(4), 321–33.
doi:10.1016/j.aanat.2011.04.008

Ydens, E., Cauwels, A., Asselbergh, B., Goethals, S., Peeraer, L., Lomet, G., ... Janssens, S. (2012). Acute injury in the peripheral nervous system triggers an alternative macrophage response. *Journal of Neuroinflammation*, 9(1), 176. doi:10.1186/1742-2094-9-176